UNIVERSIDADE FEDERAL DO RIO GRANDE DO SUL

CENTRO ESTADUAL DE PESQUISAS EM SENSORIAMENTO REMOTO E METEOROLOGIA

PROGRAMA DE PÓS-GRADUAÇÃO EM SENSORIAMENTO REMOTO

DOUGLAS GALIMBERTI BARBOSA

DETECÇÃO DE POLUIÇÃO PLÁSTICA POR MEIO DE MODELOS DE TRANSFERÊNCIA RADIATIVA E APRENDIZADO DE MÁQUINA

PORTO ALEGRE

2024

Douglas Galimberti Barbosa

Detecção de Poluição Plástica por Meio de Modelos de Transferência Radiativa e Aprendizado de Máquina

Dissertação de mestrado apresentada ao Programa de Pós-Graduação em Sensoriamento Remoto como requisito parcial para a obtenção do título de mestre em Sensoriamento Remoto e Geoprocessamento.

Orientador: Prof. Dr. Cristiano Lima Hackmann

PORTO ALEGRE

2024

CIP - Catalogação na Publicação

Galimberti Barbosa, Douglas
Detecção de poluição plástica por meio de modelos de transferência radiativa e aprendizado de máquina / Douglas Galimberti Barbosa. -- 2024.
51 f.
Orientador: Cristiano Lima Hackmann.

Dissertação (Mestrado) -- Universidade Federal do Rio Grande do Sul, Centro Estadual de Pesquisas em Sensoriamento Remoto e Meteorologia, Programa de Pós-Graduação em Sensoriamento Remoto, Porto Alegre, BR-RS, 2024.

1. poluição plástica. 2. transferência radiativa. 3. índices radiométricos. 4. sensoriamento remoto orbital. 5. gerenciamento costeiro. I. Lima Hackmann, Cristiano, orient. II. Título.

Elaborada pelo Sistema de Geração Automática de Ficha Catalográfica da UFRGS com os dados fornecidos pelo(a) autor(a).

Dedico este trabalho à minha família e amigos. A vida só faz sentido quando partilhamos nossos desejos e conquistas.

AGRADECIMENTOS

Ao Programa de Pós-Graduação em Sensoriamento Remoto e à CAPES pela concessão da bolsa de pesquisa.

À Universidade Federal do Rio Grande do Sul pelo espaço de formação e pelas experiências enriquecedoras.

À Letícia Dias Monteiro, minha esposa e companheira de vida, que deu apoio em todos os momentos difíceis.

Ao meu orientador Cristiano Lima Hackmann pelos ensinamentos e pelo companheirismo ao longo da jornada da pós-graduação.

À Bianca Matos de Barros pelas contribuições inestimáveis para o desenvolvimento do estudo.

Aos meus pais Humberto e Clarice por todo o amor e suporte.

Aos queridos amigos André, Bruna, Caio, Fernanda, Luísa e Natália pelo carinho e apoio.

RESUMO

A poluição por plásticos é considerada uma ameaça global para os ecossistemas marinhos e para a saúde humana. As técnicas de sensoriamento remoto são capazes de mapear grandes áreas em intervalos curtos tempo, o que torna viável a análise da poluição plástica em ambientes marinhos. Este estudo teve por objetivo principal identificar a presença de plásticos em zonas costeiras através de técnicas de sensoriamento remoto. Para isto, foram criadas simulações de ambientes aquáticos poluídos no modelo Discrete Anisotropic Radiative Transfer (DART). O sensor MultiSpectral Instrument (MSI), a bordo dos satélites Sentinel-2A/2B, foi escolhido para este estudo. Através da observação da assinatura espectral dos plásticos pelas imagens simuladas, assim como a análise da estrutura molecular dos polímeros, foi desenvolvido o Plastic-Water Differentiation Index (PWDI). Este índice radiométrico demonstrou separabilidade entre plásticos e água nas imagens simuladas. Para testar a eficácia do PWDI e compará-lo a outros índices foram empregados o algoritmo de clusterização K-means e o algoritmo de aprendizado de máquina Random Forest (RF). Um conjunto de imagens MSI/Sentinel-2 com presença confirmada de plásticos foi escolhido para aplicação dos algoritmos. A aplicação do *K-means*, realizada com um valor de $k=4$, resultou em um cluster composto por polipropileno nas imagens simuladas. O algoritmo foi capaz de discernir entre água com matéria flutuante e água pura ao incorporar o PWDI no método de clusterização. De acordo com os resultados obtidos pelo algoritmo RF, a integração de índices radiométricos em conjunto com bandas espectrais melhorou a detecção dos plásticos nas imagens MSI/Sentinel-2. O PWDI apresentou o maior impacto nas decisões do algoritmo de acordo com o cálculo de importância de *features*.

Palavras-chave: detritos marinhos, aprendizado de máquina, transferência radiativa

ABSTRACT

Plastic pollution is considered a global threat to marine ecosystems and human health. Remote sensing techniques are capable of mapping large areas in short time intervals, making it feasible to analyze plastic pollution in marine environments. This study aimed to identify the presence of plastics in coastal zones through remote sensing techniques. For this purpose, simulations of polluted aquatic environments were created using the Discrete Anisotropic Radiative Transfer (DART) model. The MultiSpectral Instrument (MSI), aboard Sentinel-2A/2B satellites, was chosen for this study. By observing the spectral signature of plastics in simulated images, as well as analyzing the molecular structure of polymers, the Plastic-Water Differentiation Index (PWDI) was developed. This radiometric index demonstrated separability between plastics and water in simulated images. To test the efficacy of PWDI and compare it to other indices, the K-means clustering algorithm and the Random Forest (RF) machine learning algorithm were employed. A set of MSI/Sentinel-2 images with confirmed presence of plastics was chosen for algorithm application. The application of K-means, performed with a value of k=4, resulted in a cluster composed of polypropylene in the simulated images. The algorithm was able to discern between water with floating matter and pure water by incorporating PWDI into the clustering method. According to the results obtained by the RF algorithm, the integration of radiometric indices together with spectral bands improved plastic detection in MSI/Sentinel-2 images. PWDI showed the greatest impact on algorithm decisions according to feature importance calculations.

Keywords: marine debris, machine learning, radiative transfer

LISTA DE ILUSTRAÇÕES

LISTA DE TABELAS

LISTA DE ABREVIATURAS E SIGLAS

LDPE	Polietileno de baixa densidade
PET	Politereftalato de etileno
PP	Polipropileno
HDPE	Polietileno de alta densidade
PA	Poliamida
MSI	MultiSpectral Instrument
NIR	Near Infrared
SWIR	Shortwave Infrared
RF	Random Forest
LDA	Linear Discriminant Analysis
SVM	Support Vector Machine
PLP	Plastic Litter Project
NDVI	Normalized Difference Vegetation Index
VANTs	Veículos Aéreos Não-Tripulados
DART	Discrete Anisotropic Radiative Transfer
PWDI	Plastic-Water Differentiation Index
FDI	Floating Debris Index
PI	Plastics Index

SUMÁRIO

1 INTRODUÇÃO

Os plásticos são materiais que revolucionaram inúmeras indústrias por sua versatilidade e durabilidade. No entanto, a proliferação dos plásticos de uso único e seu consumo insustentável acaba por gerar um influxo de resíduos depositados ativa ou passivamente no meio ambiente. A poluição por plásticos é um desafio global que afeta os ambientes de diversas maneiras. Estes detritos plásticos, resistentes, mas propensos à fragmentação sob processos naturais de intemperismo, representam uma ameaça pervasiva à vida marinha por meio de emaranhamento, ingestão e degradação do habitat (Andrady, 2011; Kuhn et al., 2015). Além disso, a poluição por plásticos afeta negativamente diversas atividades humanas dependentes de recursos marinhos, como navegação, pesca e turismo (Aretoulaki et al., 2021).

Em resposta a esta crescente crise ambiental, o uso de técnicas de sensoriamento remoto emergiu como uma ferramenta valiosa para complementar métodos tradicionais de avaliação e monitoramento da poluição por plásticos. O sensoriamento remoto oferece a vantagem de cobertura geográfica ampla, custo-efetividade e aquisição rápida de dados, tornando-se uma opção atrativa para monitorar detritos plásticos em vastas extensões oceânicas. Estudos recentes têm demonstrado a eficácia do sensoriamento remoto na detecção de aglomerados de plástico em ambientes costeiros e marinhos, embora com limitações decorrentes principalmente das resoluções espaciais e espectrais dos sensores (Garaba & Dierssen, 2018; Salgado-Hernanz et al., 2021).

Um dos principais desafios na detecção baseada em sensoriamento remoto da poluição por plásticos reside em distinguir entre plásticos e água (Moshtaghi et al., 2021). O ambiente marinho é fortemente afetado pelo efeito de absorção da luz, inerente ao comportamento espectral da água. Este fato acaba por mascarar a assinatura espectral do plástico, assim como de outros alvos comuns nos oceanos, como espuma marinha, vegetação aquática e madeira (Hu, 2022). Além disso, identificar plásticos submersos ou parcialmente cobertos por água representa um obstáculo significativo, complicando sua detecção precisa (Moshtaghi et al., 2021).

Ao desenvolver métodos de detecção de plásticos, é importante considerar as diferenças nas assinaturas espectrais de plásticos virgens e de plásticos

intemperizados encontrados em ambientes marinhos (Garaba & Dierssen, 2017). Além disso, a identificação de diferentes tipos de plásticos requer a análise de suas características espectrais distintas. Atualmente, as metodologias principais para lidar com esta problemática envolvem: (i) índices radiométricos, (ii) algoritmos de aprendizado de máquina e (iii) experimentos controlados (Biermann et al., 2020; Basu et al., 2021; Moshtaghi et al., 2021). Há também casos em que múltiplas técnicas e tipos de sensores são integrados (Acuña-Ruz et al., 2018; Themistocleous et al., 2020). De maneira geral, o sensor MultiSpectral Instrument, a bordo dos satélites Sentinel-2A/2B, é o mais frequentemente utilizado por estudos de detecção de poluição por plásticos (Hu, 2022). Este sensor tem bandas multiespectrais de 10 a 20 m de resolução espacial, cobrindo o espectro do visível até o infravermelho de ondas curtas. Por estes meios, é possível a detecção das denominadas manchas de plásticos, que são objetos flutuantes com tamanhos variando de 0,2 a 10 km de comprimento, geralmente associados com macroalgas, madeira e espuma marinha (Biermann et al., 2020; Ciappa, 2021).

Uma abordagem promissora para melhorar a detecção de plásticos é o uso de modelos de transferência radiativa para simular condições ambientais complexas e gerar dados sintéticos, que tem como propósito: demonstrar o comportamento espectral da poluição por plásticos e servir como dados de treinamento para algoritmos de detecção. Como exemplo, o modelo Discrete Anisotropic Radiative Transfer (DART), escolhido para o presente estudo, permite simular a interação da luz com os objetos em cenários tridimensionais. O DART é capaz de simular qualquer configuração de sensor dentro do espectro visível até o infravermelho termal. É possível também incluir as assinaturas espectrais dos objetos presentes no cenário. Isso possibilita examinar como os sensores detectam diferentes tipos de plásticos em condições distintas.

Este estudo teve como objetivo principal mapear a presença de plásticos em zonas costeiras através de técnicas de sensoriamento remoto. Para tal, foi simulado um ambiente aquático poluído através do modelo DART, no qual foram incluídos plásticos, água e espuma marinha; estes alvos são comumente confundidos com detritos marinhos quando há o efeito de mistura espectral nas imagens de sensoriamento remoto (Biermann et al, 2020; Ciappa, 2021). Foram extraídas as informações de plásticos intemperizados da base de dados desenvolvida por

Moshtaghi et al. (2021), compostos por polietileno de baixa densidade (LDPE), politereftalato de etileno (PET) e polipropileno (PP) para compor as cenas do modelo DART. Estes alvos de plásticos foram dispostos a diferentes proporções do pixel do sensor MSI/Sentinel-2 (10 m). Os alvos foram adicionados às simulações nas condições: seco, úmido e submerso, para testar as diferenças nos valores de reflectância devido a estes fatores.

Para esclarecer algumas das decisões em relação às configurações dos experimentos do presente trabalho, deve ser levado em conta o estudo prévio desenvolvido por De Barros et al. (2021). As simulações construídas no modelo DART foram utilizadas para realizar uma análise exploratória do comportamento espectral dos plásticos. Os cenários contendo plásticos, água e areia foram examinados. A base de dados de polímeros virgens de Garaba & Dierssen (2017) foi utilizada para a construção das simulações. Houve a aplicação do algoritmo de clusterização *K-means* com diferentes configurações de cluster (k = 3, 4, 5) em imagens reais do sensor MSI/Sentinel-2. A partir das conclusões deste trabalho foi possível a análise das características espectrais dos plásticos em ambientes costeiros simulados. Foi observado que a utilização de polímeros com certo grau de degradação ambiental era necessária para o avanço da detecção de poluição plástica por sensores remotos. Ademais, no presente estudo a areia não foi incluída para que mais testes em relação à separabilidade dos plásticos e água fossem realizados.

A partir dos dados de reflectância gerados pelo modelo DART, assim como a análise da estrutura molecular dos polímeros, foi possível a criação do *Plastic-Water Differentiation Index* (PWDI). O PWDI leva em consideração as características únicas do comportamento espectral dos plásticos, para que seja possível a sua detecção no ambiente aquático, inclusive quando estão totalmente submersos. Para avaliar sua eficácia e compará-la a de outros índices que possuem o mesmo propósito, foram realizadas as aplicações de um algoritmo de clusterização não-supervisionado (*K-means*) e um algoritmo de aprendizado de máquina (*Random Forest*). A aplicação do algoritmo *K-means* nas imagens DART e em imagens MSI/Sentinel-2 com presença confirmada de plásticos está detalhada na **Seção 2.3**. Já a técnica de aprendizado de máquina *Random Forest*, que teve como dados de

treinamento as imagens DART para a classificação das imagens MSI/Sentinel-2 teve sua descrição aprofundada na **Seção 2.4**.

1.1 Objetivos

1.1.1 Objetivo geral

Mapear a presença de plásticos em zonas costeiras através de técnicas de sensoriamento remoto.

1.1.2 Objetivos específicos

- Desenvolver um índice radiométrico especializado para a detecção de plásticos parcialmente ou totalmente submersos em ambientes marinhos;
- Avaliar a eficácia e comparar o índice radiométrico desenvolvido com outros índices que possuem propósitos similares;
- Examinar o potencial do modelo de transferência radiativa DART para a identificação da assinatura espectral de poluição plástica;
- Investigar a capacidade de detecção de plásticos por um algoritmo de clusterização e por uma técnica de aprendizado de máquina.

2 DESENVOLVIMENTO

O desenvolvimento do presente estudo é apresentado na **Seção 2.1** com a descrição do estado da arte sobre os trabalhos de sensoriamento remoto aplicados à poluição por plásticos. A **Seção 2.2** apresenta de maneira resumida todos os passos metodológicos para a realização deste trabalho. Todos os materiais utilizados, métodos empregados e os resultados detalhados desta pesquisa estão descritos pelos artigos científicos localizados nas **Seções 2.3** e **2.4**.

2.1 Referencial teórico

A poluição por plásticos é uma complexa problemática ambiental no que diz respeito às diferenças entre os materiais depositados no meio ambiente. Cerca de 8 milhões de toneladas de plásticos chegam aos oceanos todos os anos (Jambeck et al., 2015). A maior parte dos plásticos coletados em oceanos e rios é composta por polietileno (LDPE, HDPE), enquanto o polipropileno (PP) é o segundo polímero mais abundante (Schwarz et al., 2019; Zheng et al., 2020). Estes polímeros são comumente empregados para a fabricação de itens como sacolas plásticas, embalagens e outros produtos de uso único (Magrini, 2012). Outro fator que impacta na expressividade destes polímeros é sua densidade específica.

Tabela 1. Densidade específica de polímeros (adaptada de Campanale et al., 2020).

Polímero	Abreviação	Densidade específica (g/cm³)
Poliestireno	PS	0.01 - 1.06
Polipropileno	PP	0.85 - 0.92
Polietileno de baixa densidade	LDPE	0.89 - 0.93
High-density polyethylene	HDPE	0.94 - 0.98
Poliamida/Nylon 6.6	PA/PA 6.6	1.12 - 1.15
Policarbonato	PC	1.20 - 1.22
Poliuretano	PU	1.20 - 1.26
Tereftalato de polietileno	PET	1.38 - 1.41
Cloreto de polivinila	PVC	1.38 - 1.41
Politetrafluoretileno	PTFE	2.10 - 2.30

Tabela 2. Densidade específica da água (adaptada de Campanale et al., 2020).

Fluido	Densidade específica (g/cm³)
Água	1.00
Água do mar	1.02

Cerca de 70% dos plásticos acabam por afundar nos oceanos devido aos efeitos de bioincrustação e lastro (Pham et al., 2014). A bioincrustação é o processo pelo qual organismos marinhos, como algas, bactérias, moluscos e crustáceos, aderem à superfície dos plásticos, formando uma camada biológica que os leva a afundar. Já o lastro ocorre quando os plásticos flutuantes acumulam sedimentos ou outros materiais pesados em sua superfície, aumentando sua densidade e contribuindo para seu afundamento nos oceanos. Estes fatores somados às diferentes densidades específicas de cada polímero impactam na dispersão dos mesmos em ambientes naturais. Como exemplo, redes de pesca perdidas, denominadas como redes fantasmas, são materiais geralmente compostos por poliamida (PA), HDPE e PET; isto resulta em uma densidade específica neutra com relação a água, fazendo com que as redes fantasmas sejam carregadas por correntes marítimas, potencialmente causando emaranhamento da biota marinha (Bertelsen & Ottosen, 2016). Ademais, a detecção de detritos marinhos por sensores remotos e os esforços de coleta deste material também podem ser impactados por esta diferença na densidade. LDPE, HDPE e PP são polímeros com densidade específica menor que a da água (Tabela 1 e 2). Portanto, para os estudos de sensoriamento remoto com foco em detectar plásticos na superfície de corpos d'água, estes polímeros são de grande relevância.

Com relação ao atual estado da arte na detecção de poluição plástica em ambientes marinhos por sensoriamento remoto, há grande necessidade de (i) compreensão sobre a interação da luz com polímeros e (ii) o desenvolvimento de dados de verdade de campo. A fim de desenvolver e melhorar as técnicas de sensoriamento remoto atuais, que visam detectar plásticos com base em suas assinaturas espectrais únicas, é essencial compreender sua estrutura molecular. As propriedades dos plásticos dependem de seus respectivos polímeros. Os polímeros

são grandes moléculas compostas principalmente ou inteiramente por numerosas unidades estruturais semelhantes que estão ligadas por um processo denominado polimerização (Jansen, 2016). Como exemplo, o polipropileno é um plástico comercialmente popular formado pela polimerização de moléculas de propileno (cadeias de carbono-hidrogênio).

Tasseron et al. (2021) analisaram amostras de plásticos virgens e verificaram que as características de absorção mencionadas em estudos anteriores originavam-se da absorção de luz pelas cadeias moleculares. Essa absorção causava a transição das cadeias de um estado fundamental para um estado excitado, ocorrendo em cinco níveis distintos. Os dois primeiros níveis correspondiam às faixas de comprimento de onda de 950-1600 nm, correspondentes ao infravermelho próximo, do inglês *Near Infrared* e ao infravermelho de ondas curtas, do inglês *Shortwave Infrared* (NIR e SWIR), os quais apresentavam os maiores saltos de energia, resultando em características de absorção mais fortes. No entanto, a maioria das assinaturas espectrais de plástico apresentam um pico de reflectância em torno do comprimento de onda de 833 nm (Garaba & Dierssen, 2018; Biermann et al., 2020). Isso se deve às ligações de hidrogênio (como C-H, N-H e O-H) que absorvem e dispersam luz na região do NIR, resultando em picos de absorção mais amplos e menos intensos (Papini, 1997).

É possível observar através das bibliotecas espectrais desenvolvidas por estudos controlados em laboratórios que as estruturas moleculares dos polímeros desempenham um papel importante na definição do seu comportamento espectral (Garaba & Dierssen, 2017; Acuña-Ruz et al., 2018; Dierssen & Garaba, 2020). O estudo desenvolvido por Moshtaghi et al. (2021) ampliou o conhecimento sobre as assinaturas espectrais do plástico ao produzir um banco de dados que consiste em 47 tipos de plásticos marinhos coletados no porto de Antuérpia, Bélgica. Um dispositivo analítico hiperespectral foi utilizado em um ambiente de laboratório controlado para extrair os espectros dos plásticos imersos em água a diferentes profundidades. Entre as descobertas do estudo, foi solidificada ainda mais a presença de picos notáveis de absorção de luz especificamente na região NIR-SWIR (1070, 1213, 1470 e 1730 nm). O estudo destaca a notável disparidade entre as assinaturas espectrais do plástico. Também é demonstrado que os valores de

reflectância dos plásticos molhados e submersos são reduzidos devido ao coeficiente de absorção de luz da água, que tem um grau variável de eficácia dependendo da capacidade do plástico de absorver umidade. Este foi considerado como um dos bancos de dados mais abrangentes até o momento, devido às diversas situações em que os plásticos foram analisados.

Além das técnicas laboratoriais, os estudos de sensoriamento remoto que investigam esta problemática desenvolveram índices radiométricos com o objetivo de detectar plásticos no ambiente marinho. Biermann et al. (2020) desenvolveram o *Floating Debris Index* (FDI), que utiliza a banda espectral NIR, do sensor MSI, como principal fator para detectar os plásticos. Os resultados demonstraram que o uso do FDI em conjunto com o *Normalized Difference Vegetation Index* (NDVI) e a classificação supervisionada do algoritmo Naïve-Bayes tiveram uma acurácia de 86% na identificação de manchas de plásticos em 6 zonas costeiras diferentes. No entanto, como demonstrado por Moshtaghi et. al (2021), a replicação dos resultados alterando fatores como a cor, a profundidade e o tipo de polímero impossibilitaram a correta detecção pelo índice. Além disso, o trabalho desenvolvido por Themistocleous et al. (2020) resultou no Plastics Index, que também utiliza a banda espectral NIR. O estudo demonstrou a eficácia do índice em detectar alvos de plásticos construídos e ancorados em uma zona costeira do Chipre. Foi utilizado o sensor MSI em conjunção com veículos aéreos não-tripulados (VANTs) para a obtenção dos resultados. Além do índice, o estudo também produziu dados de verdade de campo, através de pixels com a presença confirmada de plástico. Em uma linha similar, o *Plastic Litter Project* (PLP), desenvolvido pela *University of Aegean*, Grécia, vem desde o ano de 2018 construindo diversos alvos retangulares compostos por diversos polímeros (Topouzelis et al., 2020; Papageorgiou et al., 2022). Estes alvos foram ancorados no mar na tentativa de cobrir 100% do pixel do sensor MSI (10 m). A elaboração deste tipo de estudo é de suma importância para que outros trabalhos possam vir a validar as técnicas de sensoriamento remoto empregadas.

Estudos recentes têm mostrado resultados promissores na identificação de plásticos utilizando algoritmos de aprendizado de máquina, índices espectrais, análise das assinaturas espectrais do plástico, ou uma combinação dessas

metodologias (Salgado-Hernanz et al., 2021). Os problemas mais comuns encontrados por estudos desta área do conhecimento são: distinguir plásticos de tamanho menor, plásticos submersos, falta de dados para validação, limitações de resolução espectral, temporal ou espacial dos sensores ópticos (Martínez-Vicente et al., 2019; Hu, 2022). O modelo DART tem o potencial para gerar produtos de sensoriamento remoto que possam suprir a necessidade de dados de validação ou dados de treinamento (Gastellu-Etchegorry et al., 2012; De Barros et al., 2021). Ademais, a proposta do índice (PWDI) desenvolvido pelo presente estudo é a detecção de plásticos totalmente submersos na coluna d'água.

Embora técnicas de aprendizado de máquina demonstrem potencial para detectar plásticos, alguns estudos destacam certas limitações em seu desempenho (Gonçalves et al., 2020; Aleem et al., 2022). Estas limitações estão relacionadas à obtenção de altos níveis de precisão, dificuldade em adaptar modelos a ambientes ou condições desconhecidas, e problemas com falsos positivos ou falsos negativos. Acuña-Ruz et al. (2018) compararam os algoritmos *Random Forest* (RF), Análise Discriminante Linear (LDA) e Máquina de Vetores de Suporte (SVM) para detectar resíduos de plástico, mais especificamente caixas de poliestireno em uma praia. Eles conseguiram obter uma precisão superior a 75% usando RF e LDA, e a maior precisão de 90% usando SVM. Basu et al. (2021) combinaram algoritmos não supervisionados (K-means e Fuzzy C-means) e supervisionados (Regressão de Vetores de Suporte e Fuzzy C-means Semi-supervisionado) para detectar plásticos nas imagens do Sentinel-2 apresentadas nos estudos do PLP e no estudo desenvolvido por Topouzelis et al. (2020) e Papageorgiou et al. (2022). A aplicação dos algoritmos foi capaz de alcançar precisões muito altas, de até 98,4%, mas resultou em problemas com falsos negativos em relação à detecção do plástico.

Com relação à utilização de modelos de transferência radiativa para a análise desta problemática, há poucos exemplos a serem analisados. Garaba & Harmel (2022) empregaram o modelo 6SV para simular o sinal de plásticos submersos detectados a nível de topo de atmosfera pelos sensores dos satélites Worldview-3, Sentinel-2 e Sentinel-3. O estudo concluiu que plásticos submersos acima de 1 metro na coluna d'água podem ser detectados. Já Kuester & Bochow (2019) aplicaram o modelo HySimCar para simular um sensor hiperespectral e analisar os

efeitos da transparência dos plásticos. Estes trabalhos, embora usem modelos de transferência radiativa, tiveram objetivos e técnicas distintas do presente estudo.

2.2 Metodologia

De forma a sumarizar a metodologia empregada no presente estudo, o fluxograma apresentado na Figura 1 foi desenvolvido. O primeiro passo consistiu na simulação de uma zona costeira com poluição por plásticos através da utilização do modelo DART. O sensor MSI/Sentinel-2 teve suas configurações importadas para o modelo de transferência radiativa. Foram extraídas e processadas as assinaturas espectrais de plásticos da base de dados de Moshtaghi et al. (2021), que continha 47 assinaturas espectrais de polímeros a diferentes condições. Os polímeros selecionados foram LDPE, PET, e PP nas cores laranja e branco. A escolha dos polímeros foi devido à abundância dos mesmo quando encontrados em ambientes naturais (Schwarz et al., 2019). Por fim, as cores laranja e branco foram devido ao valor mais elevado de reflectância próximo à banda do vermelho (B4 - MSI/Sentinel-2) e aos valores mais elevados de reflectância em todo o espectro visível, respectivamente, sendo um teste inicial para verificar a diferença entre essas cores.

Os alvos de plásticos foram construídos no modelo DART e distribuídos nas cenas preenchendo 100%, 80%, 60% e 40% dos pixels com presença de água. Já nas cenas contendo espuma marinha, foram dispostos a 80%, 60% e 40%. Estas porcentagens de pixel foram escolhidas a partir de testes realizados em De Barros (2023), onde foi verificado que a inclusão de mais porcentagens acabou por aumentar o tempo computacional sem produzir dados expressivos que compensam esta aplicação. A partir dos produtos de reflectância do modelo DART e da análise das características da estrutura molecular dos polímeros, foi possível o desenvolvimento do índice radiométrico *Plastic-Water Differentiation Index* (PWDI). Este índice visa a detecção de plásticos com total submersão na coluna d’água.

Figura 1 - Fluxograma de todos os processos envolvidos na metodologia do estudo.

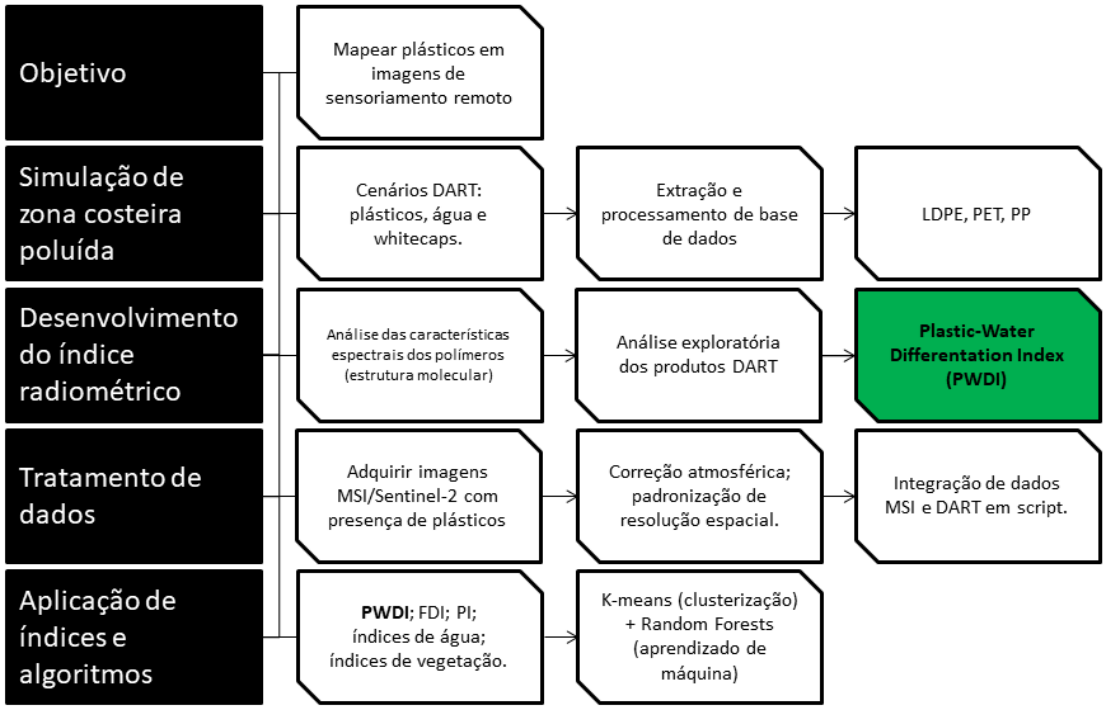

Fonte: próprio autor.

Posteriormente, foram adquiridos dados de imagens reais do sensor MSI/Sentinel-2 que continham a presença confirmada de plásticos. Para tal, foram utilizadas as imagens apresentadas no *Plastic Litter Project* (PLP), de Topouzelis et al. (2020) e Papageorgiou et al. (2022). Este grupo de pesquisas desenvolveu alvos quadrangulares preenchidos com diferentes polímeros e ancoraram-nos à deriva em duas orlas marítimas na ilha de Lesbos, Grécia (Figura 2). Estes alvos variam desde 5 até 20 m² de área. No total, 10 produtos nível 1C do sensor MSI/Sentinel-2 foram adquiridas de forma gratuita nas plataformas *United States Geological Service* (USGS) e *Copernicus Access Hub*. As imagens passaram por correção atmosférica através do algoritmo *Atmospheric Correction for OLI Lite* (ACOLITE), o qual foi escolhido por ser adequado para aplicação em áreas com presença de corpos d'água (Vanhellemont & Ruddick, 2016).

Figura 2 - Mapa de localização do local de ancoragem dos alvos de plástico do projeto PLP.

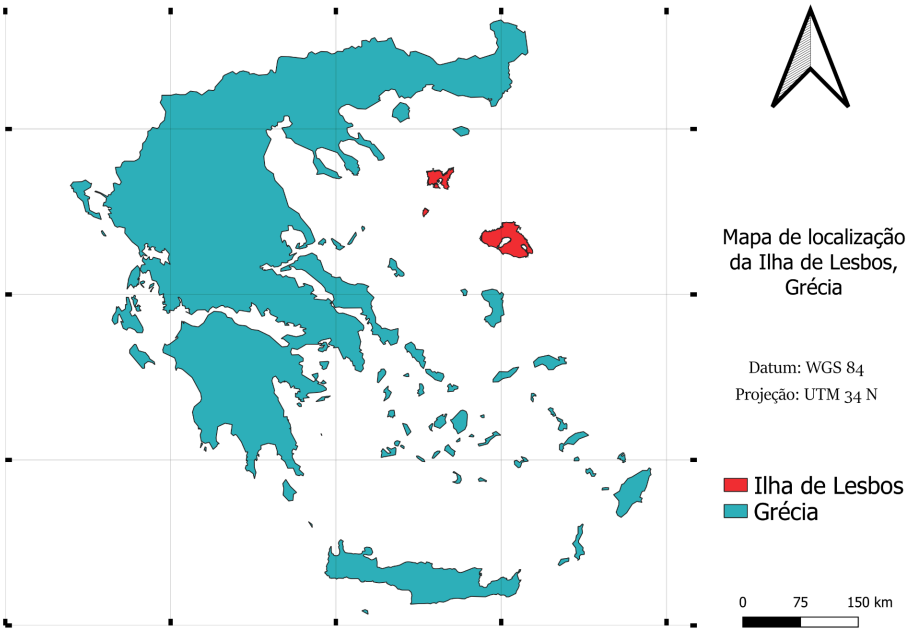

Fonte: próprio autor.

Em seguida, os produtos do modelo DART e MSI/Sentinel-2 foram padronizados através da função *Resampling* utilizando a linguagem de programação Python. Todas as imagens com 20 metros de resolução espacial foram reamostradas para 10 metros através do método de interpolação bilinear, o qual gerou a menor amplitude em relação aos dados observados de acordo com De Barros (2023).

Após a etapa de tratamento de dados, houve a aplicação dos índices radiométricos, visando testar seu potencial em detectar plásticos tanto nas imagens simuladas quanto reais. Para comparar a eficácia do PWDI em relação a outros índices similares, o *Floating Debris Index* (FDI), de Biermann et al. (2020), e o *Plastics Index* (PI), de Themistocleous et al. (2020), foram aplicados. Índices de detecção de corpos d'água e vegetação também foram incluídos para verificar seu impacto na detecção dos alvos.

Por fim, foram implementados os algoritmos *K-means* e *Random Forest*. O algoritmo de clusterização *K-means* foi aplicado tanto nas imagens DART quanto nas imagens MSI/Sentinel-2. Este método de clusterização foi escolhido por sua robustez, facilidade de implementação e potencial para agrupar grandes conjuntos de dados. Se comparado com modelos como mistura gaussiana ou clusterização hierárquica, o *K-means* é menos intensivo computacionalmente e, portanto, adequado para o objetivo deste estudo. A configuração de $k = 4$ foi selecionada com base nos testes realizados por De Barros (2023), onde foi verificado que este é o valor ideal quanto ao balanço entre *clusters* para as classes presentes nas imagens se comparado a $k = 3$ e $k = 5$. A técnica de aprendizado de máquina RF foi selecionada por sua robustez em relação à classificação de conjuntos de dados desbalanceados, o que é o caso tanto das imagens DART quanto as imagens MSI/Sentinel-2 com presença de plásticos. Ademais, o RF fornece gráficos com o cálculo de importância de cada *feature* utilizada para a classificação, o que é de suma importância para interpretar o impacto dos índices radiométricos analisados. Os dados de treinamento utilizados foram as imagens sintéticas do modelo DART. Deste modo, as imagens MSI/Sentinel-2 foram classificadas entre “plástico” e “água”.

2.3 DEVELOPMENT OF A NOVEL PLASTIC-WATER DIFFERENTIATION INDEX FOR DETECTING PLASTIC DEBRIS IN SENTINEL-2 IMAGERY

Douglas Galimberti Barbosa[1*] Bianca Matos de Barros, Cristiano Lima Hackmann

[1] Lab. of Remote Sensing of Coastal and Urban Environments (RESCUE), Brazil - UFRGS/PPGSR

KEY WORDS: plastic debris detection, spectral signature analysis, environmental monitoring, marine pollution

ABSTRACT:

Plastic pollution is a major concern in marine ecosystems. Plastics are a class of polymers that are widely distributed in marine environments, and their spectral signatures can be used to distinguish them from water. In this study, we developed a novel Plastic-Water Differentiation Index (PWDI) based on a comprehensive analysis of plastic spectral signatures. We designed simulations of a plastic polluted coastal zone by applying the Discrete Anisotropic Radiative Transfer (DART) model. Furthermore, we selected Sentinel-2 images with confirmed plastic presence in order to test our spectral index. The PWDI revealed separability between plastic and water pixels in a simulated scenario. The proposed index exhibited a potential to detect submerged polypropylene (PP) on DART simulations. The K-means unsupervised clustering algorithm was applied to simulated images and was able to create a plastic cluster composed of White PP. Its application on the remote sensing images resulted in clusters of pure water and water with floating matter. Based on the data, the PWDI had a positive impact on the detection of water with floating plastic litter on Sentinel-2 images.

1. INTRODUCTION

Plastics are artificial materials that are used to manufacture many different products that are present in our daily lives. However, with the advent of single-use utensils and other disposable plastics, a significant fraction of the global yearly production of plastics is carried by rivers, wastewater, and winds, eventually reaching coastal and marine environments around the world [Jambeck et al., 2015]. Plastics are resistant materials, however, they undergo fragmentation due to natural weathering processes, ultimately transforming into what is commonly referred to as microplastics [Magrini, 2012, Masry et al., 2021]. Marine species have reportedly been impacted by entanglement in fishing nets, smothering in plastic bags, and also accidental ingestion of plastic particles, which causes internal injuries and poisoning [Wilcox et al., 2015, Kühn et al., 2015, Andrady, 2011]. Aside from the impacts caused to marine organisms, plastic debris also negatively affects human activities such as shipping, fishing, aquaculture, tourism and recreation [Aretoulaki et al., 2021].

In order to assess the plastic pollution issue, remote sensing techniques are becoming valuable to complement the existing methods that aim to analyse the current situation of marine debris along coastal zones and oceanic waste patches [Garaba and Dierssen, 2018, Salgado-Hernanz et al., 2021]. Because of its potential to cover wide geographical scales, its cost-effectivenes, and the frequent rate at which data is produced, it provides many advantages for monitoring plastic pollution. Recent studies have succesfully detected plastic patches in both coastal and marine environments [Amézquita Toledo et al., 2017, Biermann et al., 2020]. However, there are certain limitations regarding mainly the sensors' spatial and spectral resolutions [Hu, 2022]. Even with the latest methods available, identifying plastics that are wet or submerged remains a challenging task, as well as distinguishing between the different types of plastics [Moshtaghi et al., 2021]. Also, commonly found targets, such as sea foam - also known as whitecaps - can hinder the correct identification of plastics [Biermann et al., 2020, Dierssen and Garaba, 2020]. For the purpose of addressing these constraints, radiative transfer simulations can be employed to produce synthetic data for the purpose of evaluating and validating detection algorithms. This approach also allows for the examination of the detection limits and differentiation capabilities of plastic pollution and other targets.

In this study, we embarked on an exploratory examination of the spectral signatures of marine plastic pollution, aiming to discern promising features for its detection in coastal zones. We have chosen a spectral database that covers a range of plastics in different conditions, such as immersion at various depths and diverse polymer compositions. Plastics that are collected in aquatic environments have distinct spectral signatures from virgin plastics, due to suffering natural weathering [Garaba and Dierssen, 2017, Moshtaghi et al., 2021]. The selected database more accurately represents the spectral signatures of accumulated plastics in natural settings.

We applied the Discrete Anisotropic Radiative Transfer model (DART), to craft intricate three-dimensional scenarios. This model provides a robust framework to simulate light interaction with any material, being able to portray complex environmental conditions accurately. It models the anisotropic nature of light scattering, simulating scene components inside of 3D cubes, called "voxels" [Gastellu-Etchegorry et al., 2012]. It also allows for the creation and customization of 3D objects. We created scenes that simulate a coastal environment with the presence of floating and submerged plastic litter. Three prominent commercial plastic polymers were integrated into our simulated scenes: polypropylene (PP), low-density polyethylene (LDPE), and polyethylene terephthalate (PET). Calibration of the MultiSpectral Instrument (MSI) sensor configurations within the DART model enabled the generation of synthetic reflectance products. The plastics were set on the DART scenes, cov-

*Corresponding author: galimbertidouglas@gmail.com

ering different pixel proportions. By analysing the data produced by the radiative transfer model, as well as the scientific literature on plastic spectral signatures, we developed a novel Plastic-Water Differentiation Index (PWDI) to discern between water and plastic pixels. To evaluate its efficacy, we used MSI/Sentinel-2 imagery with confirmed instances of plastic pixels. By applying the K-means unsupervised clustering algorithm we were able to demonstrate the potential of the PWDI as a tool in remote sensing-based plastic pollution monitoring strategies.

2. PLASTIC SPECTRAL CHARACTERISTICS

There is currently a need to analyse how plastics interact with light, in order to develop and improve the current remote sensing techniques which aim to detect plastics based on their unique spectral signatures. Therefore, it is essential to understand their molecular structure. The properties of plastics depend on their respective polymer. Polymers are large molecules composed primarily or entirely of numerous similar structural units that are joined together by a process called polymerization [Jansen, 2016]. As an example, polypropylene is a commercially popular plastic that is formed by the polymerization of propylene molecules (Carbon-Hydrogen chains) [Lotz et al., 1996].

Tasseron et al. (2021) analysed virgin plastic samples and verified that the absorption characteristics mentioned in previous studies originated from the absorption of light by the molecular chains. This absorption caused the chains to transition from a ground state to an excited state, occurring on five distinct levels. The first and second levels corresponded to the 950-1600 nm (NIR-SWIR) wavelength ranges and had the largest jumps in energy level, with consequently stronger absorption features. However, the majority of plastic spectral signatures present a reflectance peak around the 833 nm wavelength [Garaba and Dierssen, 2017, Goddijn-Murphy and Dufaur, 2018]. This pertains to the hydrogen bonds (such as C-H, N-H, and O-H) that absorb and scatter light in the NIR region and result in broader and less intense absorption peaks [Papini, 1997].

It is possible to observe by available spectral libraries that the polymer molecular structures play a large role in defining their spectral behavior [Garaba and Dierssen, 2017, Acuña-Ruz et al., 2018, Dierssen and Garaba, 2020]. The study developed by Moshtaghi et al. (2021) expanded upon the insights about plastic spectral signatures by producing a database that consists of 47 types of marine plastics collected in the port of Antwerp, Belgium. A hyperspectral analytical device was used on a controlled laboratory environment to extract the spectra of plastics at different depths, with distinct polymer compositions, vegetation, and water with and without sediment concentration. Among the study's findings, it further solidified the presence of notable light absorption peaks specifically in the NIR-SWIR region (1070, 1213, 1470, and 1730 nm). The study points out the notable disparity between the plastic spectral signatures, as can be seen in Figure 1. It is also demonstrated that the reflectance values of wet and submerged plastics are lowered due to the light absorption coefficient of water (ACW), which has a varying degree of effectiveness depending on the plastic's capacity to absorb moisture. This was considered as one of the most comprehensive databases so far, because of the varied situations in which plastics were analysed.

A challenge found by researchers to correctly identify plastic in marine waste patches is the low density of the drifting materials

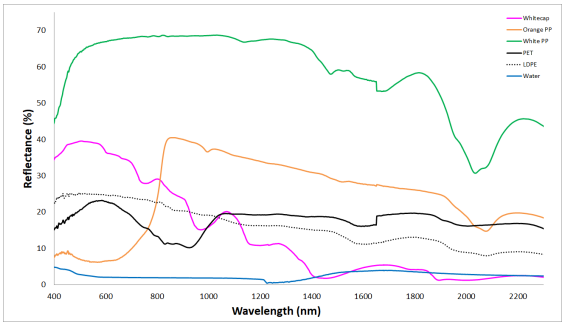

Figure 1. Plastic spectral signatures [Moshtaghi et al., 2021]; whitecap spectral signature [Dierssen, 2019]; ocean water spectral signature [Meerdink et al., 2019].

[Magrini, 2012, Dierssen and Garaba, 2020]. Marine floating debris is generally smaller ($< 10\%$) than the pixel size of the MSI/Sentinel-2 sensor, which has 10 and 20 m of spatial resolution [Hu, 2022]. For this reason, some pioneering studies decided to focus on washed ashore marine litter, which facilitates the matter of validation [Aoyama, 2014, Amézquita Toledo et al., 2017].

Recent studies have shown promising results in the identification of plastics by using machine learning algorithms, spectral indices, analysing plastic spectral signatures, or by using a mixture of these methodologies [Salgado-Hernanz et al., 2021]. However, some of the most notable limitations found are: distinguishing smaller-sized or submerged plastics from other targets, lack of ground-truth data, lack of diverse datasets, and spectral, temporal, or spatial resolution limitations of optical sensors [Martínez-Vicente et al., 2019, Hu, 2022]. Although supervised and deep learning algorithms exhibit potential for detecting plastics, a few studies highlight certain drawbacks in their performance [Gonçalves et al., 2020, Aleem et al., 2022]. These drawbacks are related to attaining high levels of accuracy, struggling to adapt models to unfamiliar environments or conditions, and problems with false positives or false negatives. To exemplify this matter, Biermann et al. (2020) have developed the Floating Debris Index (FDI), which was successful in detecting floating plastic patches along coastal zones in different areas. However, it was proven difficult to replicate the results when some factors such as polymer type, color, and depth were altered [Moshtaghi et al., 2021].

One of the main difficulties of validating the presence of plastics in remote sensing images is the scarcity of high-quality ground-truth data available in sufficient quantity. The University of Aegean has created the Plastic Litter Project (PLP) to address this issue [Topouzelis et al., 2019]. In this project, plastic targets of different sizes were constructed to ensure that they cover 100% of the MSI/Sentinel-2 pixel (10 x 10 m). Also, targets composed of wooden planks were Projects like the PLP are crucial for providing standardized testing environments for evaluating remote sensing methods and algorithms while also characterizing the types of plastics present in marine environments.

3. MATERIALS AND METHODS

This study's methodology is comprised of four main phases: (i) conducting radiative transfer simulations using the DART model, (ii) obtaining USGS images with verified plastic pixels,

(iii) creating a plastic index using the collected data, and (iv) applying an unsupervised clustering algorithm to identify plastics on the DART and USGS images. In the following subsections, each of these steps will be described in detail.

3.1 Radiative transfer simulations

The initial step in this study involved selecting a database containing plastic spectral signatures. To accomplish this, we employed the data set developed by Moshtaghi et al. (2021), which provided a comprehensive collection of spectral signatures for various plastic materials under diverse conditions. This dataset was selected because it allows for the simulation of plastics spectral signatures with natural weathering effects from being accumulated in the environment. The spectral signatures of three common commercial polymers, namely low-density polyethylene (LDPE), polyethylene terephthalate (PET), and polypropylene (PP), were selected and extracted from the database. PP samples were selected in the colors white and orange, while LDPE and PET are translucent. Subsequently, the selected spectral signature files were converted and integrated into the spectral database of the Discrete Anisotropic Radiative Transfer (DART) model.

To construct a simulated natural environment, two additional spectral signatures were selected. Firstly, a spectral signature representing oceanic water was chosen from the DART built-in spectral library to depict water without the presence of sediments or organic materials. The original source of the water spectral signature is from the ECOSTRESS spectral library [Meerdink et al., 2019]. Secondly, a spectral signature for whitecaps was simulated based on the study conducted by Dierssen et al. (2019). In this study, a third-degree polynomial equation, described in Equation (1), was employed to calculate the mean value of *in-situ* whitecap spectral signatures, providing a representative average value for reflectance encountered in marine environments.

$$\begin{aligned} R_f &= 0.47x^3 - 1.62x^2 + 8.66x + 31.81 \\ x &= \log(\alpha_w) \\ \alpha_w(m^{-1}) &= \text{Absorption coefficient of water.} \end{aligned} \tag{1}$$

The sensor chosen for this study is the MultiSpectral Instrument (MSI), equipped on the Sentinel-2A and Sentinel-2B satellites, which are part of the Copernicus program by the European Space Agency. This sensor contains 13 spectral bands ranging from VIS to SWIR, with each band ranging from 10 to 60 m of spatial resolution (Table 1). The radiometric resolution is 12 bits per pixel, providing high-quality imagery suitable for various applications. These specifications of the MSI sensor were configured on the DART model simulation settings. The MSI spectral bands selected for this study ranged from $B2$ to $B12$, excluding $B9$.

Scenarios with dimensions of 1200 x 600 m were constructed by incorporating water, square-shaped plastic targets, and whitecaps. In order to standardize the spatial resolution of the DART and USGS images from 20 to 10 m, we employed the Resampling[1] function in a Python script. The bilinear interpolation mode was chosen instead of the near and cubic modes due to its lower amplitude in comparison to the other two modes, leading to a better alignment with the distribution of the USGS

[1] Source and more details: http://tinyurl.com/resampling

Table 1. MSI/Sentinel-2 specifications.

Band	Name	λ central (nm)	Spatial res. (m)
B1	Coastal Aerosol	443	60
B2	Blue	492	10
B3	Green	560	10
B4	Red	665	10
B5	Red Edge 1	704	20
B6	Red Edge 2	741	20
B7	Red Edge 3	783	20
B8	NIR	833	10
B8a	Narrow NIR	865	20
B9	Water Vapour	945	60
B10	SWIR Cirrus	1374	60
B11	SWIR 1	1614	20
B12	SWIR 2	2202	20

images. Plastic targets were placed on the water surface with consistent positions across all simulated bands and spatial resolutions. The LDPE and PET samples were in a dry state. The PP samples were the only available wet and submerged plastics at depths of 2.5 and 5.0 cm. Each sample was placed in separate DART scenes. Plastic targets were set to pixel coverages of 40%, 60%, 80% and 100% of the MSI spatial resolution (10 m). The simulations were, then, comprised of: only water; water and plastics; only whitecaps; whitecaps and plastics; only plastics. The plastic-to-pixel proportions are demonstrated in Figure (2). The synthetic images were converted from the DART file format to a text format to more easily extract the reflectance information from the pixels of interest.

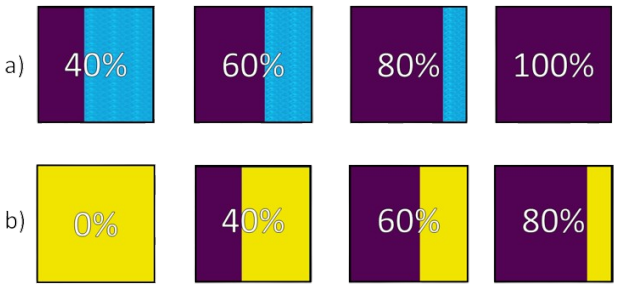

Figure 2. Plastic-to-pixel proportions on DART simulations: a) plastics are depicted in the color purple and water is depicted in the color blue, b) plastics are depicted in the color purple and whitecaps are depicted in the color yellow.

3.2 Ground-truth plastic pixels

In the subsequent phase of this research, the objective was to locate images that contained verified plastic pixels to implement the unsupervised clustering algorithm. The MSI images featured in the studies developed by the Plastic Litter Project (PLP) were selected since they contain floating plastic targets placed on the water surface of a coastal zone in Lesbos, Greece [Topouzelis et al., 2019, Papageorgiou et al., 2022]. Thus, the images contain ground-truth plastic pixels in environmental conditions which match the aim of this current study. MSI/Sentinel-2 products at level 1C were obtained from two sources: the United States Geological Survey (USGS) portal and the Copernicus Open Access Hub, ranging from years 2019 up to 2021. We refer to this set of images as "USGS images" throughout this article. To ensure precise analysis, atmospheric correction was carried out using the ACOLITE (Atmospherical Corretion for OLI Lite), applying the DSF (Dark Spectrum Fitting) algorithm, which leverages dark pixel spectra to estimate the inherent optical properties of water [Vanhellemont and

Ruddick, 2016]. ACOLITE is tailored for the challenges of removing atmospheric effects of coastal and inland water environments [Topouzelis et al., 2019]. Following that, specific areas of interest within each image were cropped using the Sentinel Application Platform (SNAP - version 8.0) software.

After processing the data, the USGS images were segmented in the following classes: plastic, coast, water, and wood. There were three main types of plastic targets present in the images, which were composed of high-density polyethylene (HDPE), LDPE, and PET.Percentual coverage of the plastic targets was estimated through visual inspection, categorized as either 100% or less than 100% (partial coverage). Geolocation data and TIFF subsets were then superimposed using QGIS (version 3.22.6) software for precise pixel mapping. A Python script was employed to integrate spatial and spectral data, labeling pixels with 100% water coverage, and those containing any percentage of plastic were designated as "Plastic". According to Topouzelis et al. (2020) and (2022), a total of 103 pixels have been annotated in the published studies conducted to date. The plastic targets were comprised of three main plastic polymers: low-density polyethylene (LDPE), high-density polyethylene (HDPE), and polyethylene terephthalate (PET).

3.3 Plastic-water differentiation index (PWDI)

A novel spectral index was developed based upon the analysis of spectral signatures derived from both DART simulations and USGS images, supplemented by a review of existing literature on the molecular structure and resulting spectral characteristics of plastics. Specifically, our investigation focused on identifying distinctive features within the spectral curve of plastics, namely the NIR ($B8$ - $833nm$) peak and the RedEdge ($B5, 6, 7$ - $704 - 783nm$) absorption line (Figure 1). These features were consistently observed across various sources, indicating their significance in the spectral signature of plastics [Garaba and Dierssen, 2017, Tasseron et al., 2021, Moshtaghi et al., 2021]. Motivated by this observation, we hypothesized that an index that leverages the contrast between the reflectance values at the NIR ($B8$) and the RedEdge_3 ($B7$) MSI optical bands could effectively discriminate plastic targets from water, which exhibits a slight NIR absorption characteristic. The following band arithmetic function (Equation 2) was then applied to both the simulated and real images:

$$\text{PWDI} = \frac{B8 - B7}{B8 + B7} \tag{2}$$

This approach takes into consideration the inherent spectral properties of plastics to develop a robust differentiation index tailored to the unique challenges posed by plastic detection in coastal environments.

We also employed additional spectral indices to our images to examine their characteristics and evaluate their effectiveness in identifying and distinguishing plastics from other objects. These indices are commonly used for tasks such as detecting water, vegetation, and plastics (Table 2). All indices with detailed descriptions can be found in Appendix (Section 6).

3.4 Unsupervised clustering algorithm

The K-means algorithm is an unsupervised clustering method widely employed in remote sensing image analysis for its ability to automatically partition data points into distinct clusters based on their similarities. In the present study, this algorithm was implemented using the open-source machine learning library *scikit-learn*. Firstly, we chose $k = 4$, based on empirical data from the study developed by De Barros et al. (2023), which demonstrated that it was the best balance between the number of clusters to classes from the datasets. De Barros et al. (2023) tested the configurations of $k = 3, 4, 5$. Then, we randomly picked k starting points as cluster centroids. Subsequently, the centroids are recalculated by determining the average of the data points allocated to each cluster (Equation 3).

Table 2. Spectral indices applied in the current study.

Applications	Spectral Index
Detecting water bodies	AWEI
	WRI
	NDWI
	MNDWI
Detecting and monitoring vegetation	NDVI
	RNDVI
	SR
Detecting floating plastics	FDI
	PI

$$\sum_{i=0}^{n} \min_{\mu_j \in C} \left(\|x_i - \mu_j\|^2 \right) \tag{3}$$

This process of updating assignments continues until convergence is reached, which is signaled by minimal variations in centroids or consistent cluster allocations. The algorithm was implemented on both the simulated and USGS images. The data points encompassed: (i) only optical bands; (ii) only spectral indices; (iii) both optical bands and spectral indices. These approaches will be respectively referred to as: optical band clustering (OBC), spectral index clustering (SIC), and integrated spectral clustering (ISC).

4. RESULTS AND DISCUSSION

4.1 Exploratory analysis

In total, 570 reflectance images spanning from the VIS to the SWIR spectral regions were generated by the DART model. Our analysis of the obtained data highlights both similarities and notable distinctions in the spectral characteristics between the simulated and the USGS images. Firstly, we observed that the simulated plastic spectral signatures exhibited shared RedEdge ($B5, B6, B7$ absorption lines and NIR ($B8$) reflectance peak (Figure 3). The submerged plastics exhibited the same patterns, but their reflectance values were lowered due to the ACW. This effect is also demonstrated by the pixels with progresively lower plastic coverage. Furthermore, our analysis of water spectral signatures in the DART scenes revealed slight NIR absorption and generally low reflectance values (ranging from 1 to 3%). Whitecaps, on the other hand, displayed spectral signatures similar to plastics, sharing common absorption and peak lines, albeit with slight discrepancies in the VIS and SWIR spectra.

These features were also present, to varying degrees, in the plastics identified in the USGS images. However, it's noteworthy that the reflectance values in the USGS 2019 images were notably lower (ranging from 3 to 7%) compared to the DART scenes (ranging from 10 to 60%), posing challenges in

identifying these spectral patterns (Figure 4). Interestingly, the USGS 2021 images displayed spectral signatures more akin to the DART plastics (Figure 5). While B5 exhibited a prominent absorption line, B6 and B7 did not. This discrepancy in the spectral shape can be attributed to the fact the USGS 2021 images contained high-density polyethylene (HDPE) targets [Papageorgiou et al., 2022]. HDPE is a slightly opaque plastic which has a specific permeability of about one-third to one-sixth that of LDPE, meaning it is less affected by the ACW [Hamilton, 1967].

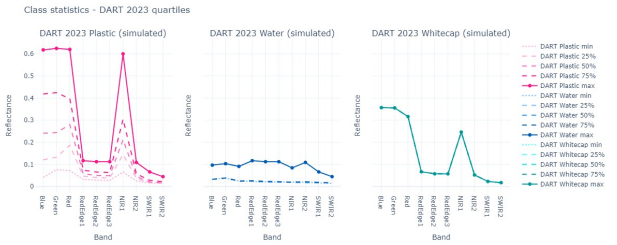

Figure 3. Class quartiles spectral signatures of DART simulations.

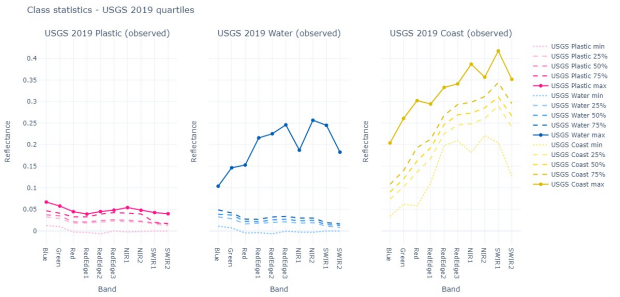

Figure 4. Class quartiles spectral signatures of USGS 2019 images.

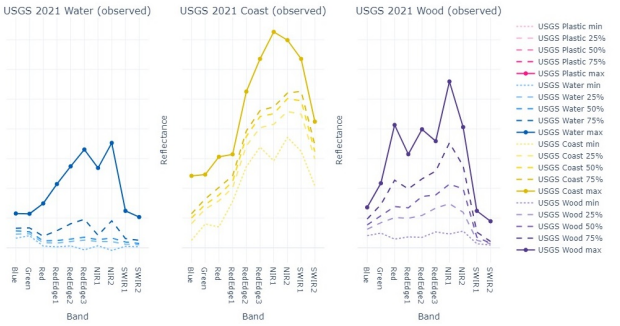

Figure 5. Class quartiles spectral signatures of USGS 2021 images.

An initial examination of the application of spectral indices in the simulated and USGS images reveals the separability between the classes in both datasets. The Floating Debris Index (FDI) had values between 0 and 0.5 in the simulated images, but grouped water, whitecaps and plastics relatively close to each other (Figure 6). As for the USGS images, the FDI had higher values, between 0.6 and 1, which were outside the range of plastics as proposed by Biermann et al. (2020). The "coast" and "wood" classes from the USGS images were also grouped relatively close to the other classes in the histograms.

The Plastics Index (PI) showed values between 0.3 and 0.55 on the simulated images, and it grouped water and whitecaps around 0.45 (Figure 7). However, plastic was distributed along this range, demonstrating a low separability between the classes. Regarding the USGS images, in the case of the 2019 images, all classes were grouped near the -0.5 values. The USGS 2021 images showed values of -0.6 to -0.4, but the classes were unevenly distributed along the entire range. Furthermore, by verifying the scatter plot graphics, there was no notable class separation between the PI and the FDI or other spectral bands or indices.

The proposed Plastic-Water Differentiation Index (PWDI) was developed based on the unique spectral features inherent to the molecular structure of plastics. The PWDI employed on the simulated images showed values between -0.6 and 0.6. All values for water were below 0 and plastic was above 0.5, demonstrating potential for separability between these two classes (Figure 8). However, whitecap was grouped near plastic in this case. Additionally, when we observed the PWDI scatter plot graphics, we encountered distribution patterns associated with the potential to separate between water and plastic pixels. As an example, on the PWDI vs RedEdge 3 scatter plot graphic, the water pixels are predominantly on the negative values of the X-axis, reflecting their characterstic spectral signatures in this band (Figure 9).

Conversely, the plastic pixels are distributed across positive values on the X-axis, indicating their distinct spectral responses. The upward slope of the plastic pixels on the graph suggests that as the PWDI values increase, the likelihood of plastic presence in the pixel also increases. The graphs's parabolic-shaped distribution pattern emphasizes the index's potential to differente between water and plastic pixels. The curvature of the parabola signifies a gradual transition between water-dominated and plastic-dominated regions, with the index's values reaching a valley at the center of the parabola, representing the optimal discrimination between the two materials. This pattern seems to be less pronounced, but still present when we observe the PET and LDPE polymers. The PWDI applied to the USGS 2019 and 2021 images showed values between 0.5 and 0.7, grouping all classes together and showing no discernible separation patterns between them.

In the simulated images, where hundreds of samples of plastic pixels were evenly distributed across different pixel coverages, the PWDI had ample data to discern the spectral signatures of plastics under various conditions. On the other hand, the limited number of plastic pixels (103 total) in the USGS images imposes constraints on the spectral analysis. With fewer samples available for analysis, the plastic spectral indices may lack the necessary data to accurately represent the spectral characteristics of plastics in real-world scenarios. The whitecap signatures, according to Moshtaghi et al. (2021), can exhibit similar spectral behavior to plastics when both are floating on the water surface. This was also the case when we looked at the simulated whitecap spectral signatures. Further investigation regarding whitecap-to-plastic pixel proportions might be necessary to be able to discern between these targets.

The USGS images are more complex and heterogeneous compared to the simulated images. They contain more land cover types, natural features, and atmospheric effects that can mask the spectral signatures of plastics. Atmospheric interference, in the form of scattering, absorption, and haze are present in real-world remote sensing images, even with the application of at-

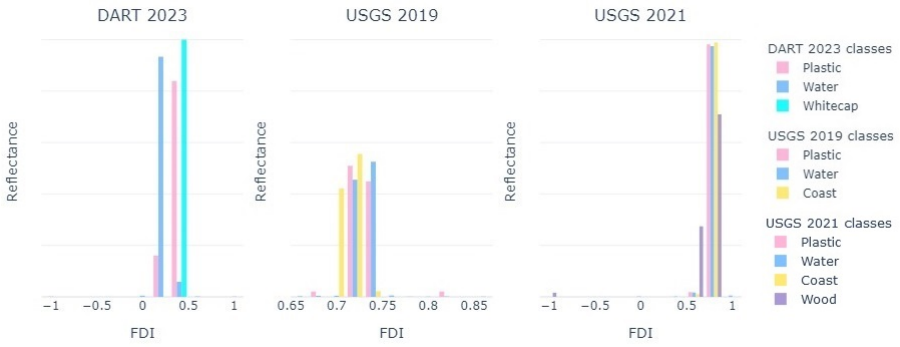

Figure 6. PWDI values distribution across classes: DART Simulations vs. 2019 & 2021 USGS imagery.

Figure 7. PI values distribution across classes: DART Simulations vs. 2019 & 2021 USGS imagery.

Figure 8. FDI values distribution across classes: DART Simulations vs. 2019 & 2021 USGS imagery.

mospheric correction algorithms. This causes a reduction in the contrast and brightness. This effect can be visualized in Figure 4, where the plastic spectral shape is flatter, and more similar to water. Nevertheless, the visible separability of dry, wet and submerged plastics from water in the simulated images by the PWDI is crucial, since plastics will be partially or fully submerged in marine pollution scenarios in many occasions. Thus, the PWDI has the potential to complement the existing indices, such as the FDI and PI, in a multi-index approach.

4.2 K-means clustering algorithm

The application of the K-means unsupervised algorithm in this study facilitated the clustering of pixels into four distinct groups, or clusters, representing different spectral characteristics. To achieve this, the initial data points were split in the three aforementioned configurations: (i) optical band clustering, (ii) spectral index clustering (the PWDI and the ones mentioned in Table 2), and (iii) integral spectral clustering. The outcomes of each configuration will be elaborated upon in the next subsections, providing a comprehensive analysis of the clustering results and the effectiveness of the applied methodology. The images in section 6.1 visually depict all polymers types assigned to each cluster in each specific approach.

4.2.1 Optical band clustering (OBC): the four resulting K-means clusters of the BC approach were able to group the DART simulated images in the following way:

Here, Cluster 0 corresponds to water located on the scene edges and right outside the close vicinity of plastics. This cluster ended up grouping some plastic pixels together with water,

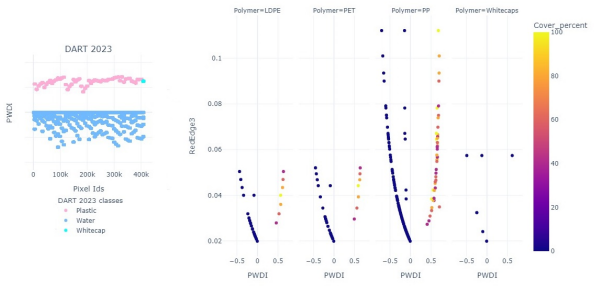

Figure 9. Class quartiles spectral signatures of USGS 2021 images.

Table 3. Simulated images OBC approach

Cluster	Water	Plastic	Whitecaps
0	376,480	512	0
1	0	2,048	0
2	0	3,968	128
3	26,240	640	0

based in their similarity. Cluster 3 is a similar case, but it corresponds to water pixels that were close to plastic or had partial plastic coverages. Cluster 1 was able to group only plastics, which is the more desired outcome. Cluster 2 grouped some polymer types together with whitecaps, since they are also somewhat similar spectral signatures.

Based on our findings, we were able to point that most polymer types were grouped in Cluster 2. Orange PP was the most prevalent polymer type in this cluster. The 60 to 80% plastic coverage range in general seems to be the one that is most confused with whitecaps by the algorithm. Cluster 0 grouped only plastic coverages of 40%, which corresponds to the least amount of pixel-to-water proportion. This might indicate a threshold for plastic detection, but it requires further experiments. Cluster 1 grouped only White PP and the 80% plastic coverage was the most numerous in this cluster. Finally, Cluster 3 mixed some Orange PP and PET pixels with water.

In the case of the USGS images, the OBC approach designated the following clusters:

Table 4. USGS images OBC approach

Cluster	Water	Plastic	Wood	Coast
0	1,519	54	6	0
1	0	0	0	440
2	1	0	6	629
3	423	49	50	0

Cluster 0 and 3 were the main water clusters, with the presence of plastics and wood. Cluster 1 and 2 contained coast pixels and a few wood and water pixels. In 5 out of 11 images, the algorithm grouped plastics on a cluster separated from water. The algorithm seems to struggle more to separate plastics from water on the 2019 images. As an example, the images from 04/18/2019 and 05/28/2019 were respectively assigned to Cluster 0 and 3 only.

The inclusion of HDPE targets on the USGS 2021 images seems to make the only bands approach somewhat better, as more plastic pixels were grouped separately from water in the images (Figure 10). Opaque plastics are generally easier to identify on remote sensing imagery, since they can stand out

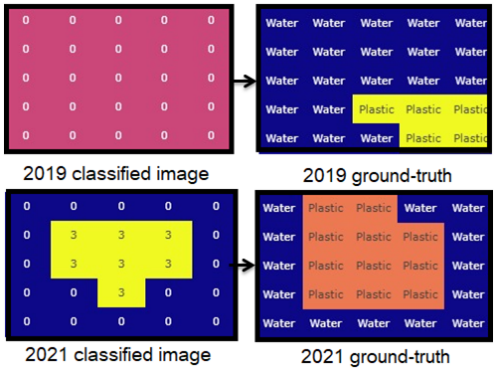

Figure 10. 2019 and 2021 USGS images clustered by K-means algorithm.

from the highly light-absorbing water, even if they are submerged. Still, the plastic's color and and specific permeability are to be taken into consideration [Moshtaghi et al., 2021].

4.2.2 Spectral index clustering (SIC): this application of the K-means algorithm used only the spectral indices from Table 2 as initial data points. It resulted in this clusterization of the simulated images:

Table 5. Simulated images SIC approach

Cluster	Water	Plastic	Whitecaps
0	18,688	0	0
1	335,520	1,280	0
2	0	5,888	128
3	48,512	0	0

Compared to the first clusterization, this one reveals notable differences. Clusters 0 and 3 contain only water. Plastics are mostly grouped on Cluster 2, but there was some mixing with water in Cluster 1. Again, whitecaps were grouped with plastics due to their similarity.

Cluster 2 contains most polymer types and all plastic coverages. White PP and LDPE pixels were entirely grouped in this cluster. Some Orange PP and PET pixels were grouped on Cluster 1. Here, the use of the spectral indices as initial data points suggests that the detection of what we refer to as "secondary water pixels", represented by clusters 1 and 3 is facilitated in this case. This can be attributed to the PWDI, FDI, and PI which were able to detect water pixels mixed with plastics and whitecaps. Whereas, the "primary water pixels" refer to pure water.

Regarding the USGS images, the SIC approach clusters were computed by the algorithm in the following manner:

Table 6. USGS images SIC approach

Cluster	Water	Plastic	Wood	Coast
0	0	0	0	397
1	1,359	64	49	0
2	1	0	0	671
3	583	39	13	1

By analysing the results of the K-means application using only indices for the USGS images, we observed that there are a few differences in the distribution of water, plastic, and wood, when comparing to the OBC approach. Plastics were slightly more concentrated on Cluster 1. Less coast pixels were grouped in Cluster 0 and 2, indicating more difficulty to separate this class. Only 1 of the images presented plastics on a separate cluster from water.

4.2.3 Integrated spectral clustering (ISC): the final step of the K-means application involved the use of all spectral bands and indices mentioned as initial data points. Following that, these were the resulting cluster in the simulated images:

Table 7. Simulated images ISC approach

Cluster	Water	Plastic	Whitecap
0	335,392	1,408	0
1	0	5,760	128
2	18,688	0	0
3	48,640	0	0

By looking at these clusterings, it is possible to notice that the values are very similar to the SIC approach. The main difference is, there are more plastic pixels being mixed with water on cluster 0. Submerged Orange PP is more numerous on Cluster 0 when compared to the previous approach. This indicates that these submerged plastics are being more confused with water in this scenario.

Finally, the clusterization of the USGS images that applied both bands and indices approach resulted in the following values:

Table 8. USGS images ISC approach

Cluster	Water	Plastic	Wood	Coast
0	0	0	0	410
1	1,359	64	49	0
2	1	0	0	659
3	583	39	13	0

The differences between the ISC and SIC approaches are negligible. Some coast pixels shifted from Cluster 2 to 0. The visual inspection of the USGS images also revelead that they are very visually similar between the two approaches. This suggests that employing both methods could produce highly comparable outcomes; however, further investigation is necessary.

The inclusion of the spectral indices, particulartly the PWDI, in the clustering approach revelead noticeable impacts. There were variations in cluster compositions on both the simulated and USGS images. In the simulated images, this led to plastics being assigned to only two clusters, in comparison to four cluster in the only bands approach. This is an indication that the PWDI can effectively distinguish between water and dry, wet, and submerged plastics, although there was more mixing between plastics and whitecaps in this context.

In the USGS images, plastics were slightly more concentrated in specific clusters. Firstly, the previously mentioned primary and secondary water pixels can be respectively interpreted as "pure water" and "water with floating matter". The spectral indices facilitated this detection of floating matter, by assigning more plastic pixels to specific clusters in conjunction with water and wood. This was most noticeable when looking at the USGS 2021 images, when HDPE-mesh was included in the study's targets [Papageorgiou et al., 2022].

The fact that the K-means algorithm groups plastics with other materials like wood and water in the USGS images, while it separates plastics from water in the simulations, suggests that the algorithm can partially detect plastics in this context. However, the inconsistency in the results indicates that there are limitations in the algorithm's ability to accurately distinguish plastics from other floating matter. Further refinement of the algorithm or consideration of additional features may be necessary to improve its performance in detecting plastics with greater reliability.

5. CONCLUSION

The comprehensive analysis of the spectral characteristics of plastics and other targets commonly appearing in coastal environments, both in simulated and real-world remote sensing images, provides valuable insights into the effectiveness and limitations of current detection methodologies. The analysis of plastic spectral signatures generated by the DART scenarios, further emphasizes that this model is a valuable tool for aiding in the detection of plastic pollution, being able to provide accurate data of distinct polymers in simulated coastal zones. Other aspects not included in the current study, such as including vegetation in the simulations, can also increase the realism created by the scenarios.

The observed similarities in spectral signatures between the simulated and USGS images underscore the potential for remote sensing techniques to detect plastics in marine environments. However, notable differences in reflectance values and clustering patterns between the two datasets highlight the challenges posed by the effects of atmospheric interference and heterogeneous surface compositions. The application of spectral indices, particularly the Plastic-Water Differentiation Index (PWDI), shows promise in distinguishing plastics from water in simulated scenarios. Nevertheless, its application in the USGS images seemed to be hindered by factors like limited sample size and the effects caused by water light absorption. The PWDI exhibited a potential to detect PP submerged at 5 cm depth according to the data. PET and LDPE are harder to detect, based on both the spectral index and clustering results. This is due to the fact that they are generally translucent plastics with lower reflectance values.

The K-means application results demonstrate the algorithm's ability to partially detect plastics. It was able to cluster White PP into a single group on simulated images, further solidifying the importance of this polymer. The threshold of 40% pixel coverage in MSI/Sentinel-2 simulated images (10 m of spatial resolution) may represent the limit beyond which plastics cannot be reliably detected, but further experiments are needed to confirm this hypothesis.

Regarding the data from the USGS images, the algorithm was effective at grouping the coast class into two distinct clusters on all the applied approaches. The separation of water and floating matter into distinct clusters indicate that the algorithm was able to distinguish between pure water and water mixed with plastics and wood. This separation was clearer both when applying the PWDI, as well as in the images that contained high-density polyethylene (HDPE). The clustering algorithm was not able to create a single cluster for plastics in the USGS images. This fact reinforces the need for refinement and additional features to enhance its effectiveness. Moreover, our data implies whitecaps are ostensibly clustered with plastics across all scenarios. In the future, we expect to refine the PWDI in order to facilitate the discrimination between whitecaps and plastics.

Overall, while remote sensing techniques hold great potential for plastic pollution detection, addressing the complexities of real-world conditions remains a crucial avenue for future research and development in this field.

6. APPENDIX

6.1 Clustering results of simulated images

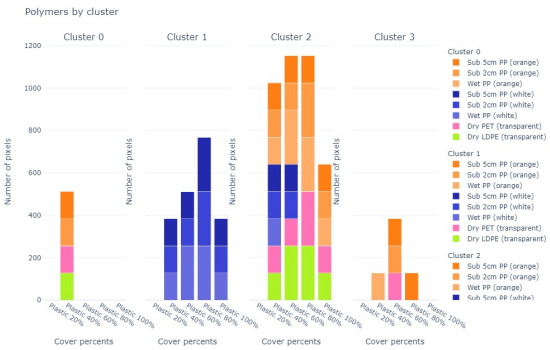

Figure 11. Number of plastic pixels allocated to each cluster using the OBC approach for the data points.

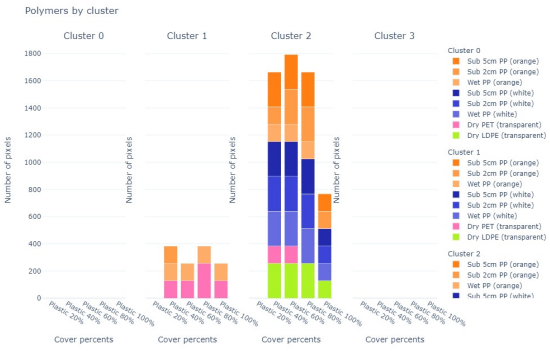

Figure 12. Number of plastic pixels allocated to each cluster using the SIC approach for the data points.

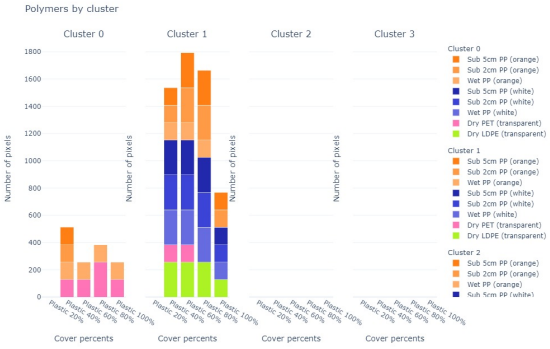

Figure 13. Number of plastic pixels allocated to each cluster using the ISC approach the data points.

6.2 Band equations of spectral indices applied in this study (expressed in terms of the MSI/Sentinel-2 bands):

Automated Water Extraction Index [Feyisa et al., 2014]

$$AWEI = 4 * (B3 - B12) - (0.25 * B8 + 2.75 * B11)$$

Water Ratio Index [Shen and Li, 2010]

$$WRI = \frac{B3+B4}{B8+B12}$$

Normalized Difference Water Index [McFeeters, 1996]

$$NDWI = \frac{B3-B8}{B3+B8}$$

Modified Normalized Difference Water Index [Xu, 2006]

$$MNDWI = \frac{B3-B12}{B4+B12}$$

Normalized Difference Vegetation Index [Rouse et al., 1974]

$$NDVI = \frac{B8-B4}{B8+B4}$$

Reversed Normalized Difference Vegetation Index [Themistocleous et al., 2020]

$$RNDVI = \frac{B4-B8}{B4+B8}$$

Simple Ratio [Jordan, 1969]

$$SR = \frac{B8}{B4}$$

Floating Debris Index [Biermann et al., 2020]

$$FDI = R_{rs,B8} - R'_{rs,B8}$$

$$R'_{rs,B8} = R_{rs,B6} + (R_{rs,B11} - R_{rs,B6})$$

$$\times \frac{(\lambda_{B8}-\lambda_{B4})}{(\lambda_{B11}-\lambda_{B4})} \times 10$$

Plastic Index [Themistocleous et al., 2020]

$$PI = \frac{B8}{B8+B4}$$

References

T. Acuña-Ruz, D. Uribe, R. Taylor, L. Amézquita, M. C. Guzmán, J. Merrill, P. Martínez, L. Voisin, and C. Mattar. Anthropogenic marine debris over beaches: Spectral characterization for remote sensing applications. *Remote Sensing of Environment*, 217:309–322, 2018.

A. Aleem, S. Tehsin, S. Kausar, and A. Jameel. Target classification of marine debris using deep learning. *Intelligent Automation & Soft Computing*, 32(1), 2022.

L. P. Amézquita Toledo et al. Elaboración de una propuesta para la gestión integral de residuos antropogénicos costeros en el archipiélado de chiloé, chile. 2017.

A. L. Andrady. Microplastics in the marine environment. *Marine pollution bulletin*, 62(8):1596–1605, 2011.

T. Aoyama. Monitoring of marine debris in the sea of japan using multi-spectral satellite images. In *Ocean Remote Sensing and Monitoring from Space*, volume 9261, page 92611E. International Society for Optics and Photonics, 2014.

E. Aretoulaki, S. Ponis, G. Plakas, K. Agalianos, et al. Marine plastic littering: A review of socio economic impacts. *J. Sustain. Sci. Manag*, 16(3):277–301, 2021.

L. Biermann, D. Clewley, V. Martinez-Vicente, and K. Topouzelis. Finding plastic patches in coastal waters using optical satellite data. *Scientific reports*, 10(1): 1–10, 2020.

B. M. de Barros, D. G. Barbosa, and C. L. Hackmann. Spectral analysis of marine debris in simulated and observed sentinel-2/msi images using unsupervised classification. *arXiv preprint arXiv:2306.15008*, 2023.

H. M. Dierssen. Hyperspectral measurements, parameterizations, and atmospheric correction of whitecaps and foam from visible to shortwave infrared for ocean color remote sensing. *Frontiers in Earth Science*, 7:14, 2019.

H. M. Dierssen and S. P. Garaba. Bright oceans: Spectral differentiation of whitecaps, sea ice, plastics, and other flotsam. In *Recent Advances in the Study of Oceanic Whitecaps*, pages 197–208. Springer, 2020.

G. L. Feyisa, H. Meilby, R. Fensholt, and S. R. Proud. Automated water extraction index: A new technique for surface water mapping using landsat imagery. *Remote sensing of environment*, 140:23–35, 2014.

S. Garaba and H. Dierssen. Spectral reference library of 11 types of virgin plastic pellets common in marine plastic debris. *Data set available on-line [http://ecosis. org] from the Ecological Spectral Information System (EcoSIS). http://dx. doi. org/10*, 21232:C27H34, 2017.

S. P. Garaba and H. M. Dierssen. An airborne remote sensing case study of synthetic hydrocarbon detection using short wave infrared absorption features identified from marine-harvested macro-and microplastics. *Remote sensing of environment*, 205:224–235, 2018.

J.-P. Gastellu-Etchegorry, E. Grau, and N. Lauret. Dart: A 3d model for remote sensing images and radiative budget of earth surfaces. *Modeling and simulation in Engineering*, pages ISBN–978, 2012.

L. Goddijn-Murphy and J. Dufaur. Proof of concept for a model of light reflectance of plastics floating on natural waters. *Marine pollution bulletin*, 135:1145–1157, 2018.

G. Gonçalves, U. Andriolo, L. Gonçalves, P. Sobral, and F. Bessa. Quantifying marine macro litter abundance on a sandy beach using unmanned aerial systems and object-oriented machine learning methods. *Remote Sensing*, 12(16): 2599, 2020.

R. Hamilton. Water vapor permeability of polyethylene and other plastic materials. *Bell System Technical Journal*, 46(2): 391–415, 1967.

C. Hu. Remote detection of marine debris using sentinel-2 imagery: A cautious note on spectral interpretations. *Marine Pollution Bulletin*, 183:114082, 2022.

J. R. Jambeck, R. Geyer, C. Wilcox, T. R. Siegler, M. Perryman, A. Andrady, R. Narayan, and K. L. Law. Plastic waste inputs from land into the ocean. *Science*, 347(6223):768–771, 2015.

J. A. Jansen. Plastics–it's all about molecular structure. *Plast. Eng*, 72(8):44–49, 2016.

C. F. Jordan. Derivation of leaf-area index from quality of light on the forest floor. *Ecology*, 50(4):663–666, 1969.

S. Kühn, E. L. B. Rebolledo, and J. A. van Franeker. Deleterious effects of litter on marine life. In *Marine anthropogenic litter*, pages 75–116. Springer, Cham, 2015.

B. Lotz, J. Wittmann, and A. Lovinger. Structure and morphology of poly (propylenes): a molecular analysis. *Polymer*, 37 (22):4979–4992, 1996.

A. Magrini. *Impactos ambientais causados pelos plásticos: uma discussão abrangente sobre os mitos e os dados científicos*. Editora E-papers, 2012.

V. Martínez-Vicente, J. R. Clark, P. Corradi, S. Aliani, M. Arias, M. Bochow, G. Bonnery, M. Cole, A. Cózar, R. Donnelly, et al. Measuring marine plastic debris from space: Initial assessment of observation requirements. *Remote Sensing*, 11 (20):2443, 2019.

M. Masry, S. Rossignol, J.-L. Gardette, S. Therias, P.-O. Bussière, and P. Wong-Wah-Chung. Characteristics, fate, and impact of marine plastic debris exposed to sunlight: A review. *Marine Pollution Bulletin*, 171:112701, 2021.

S. K. McFeeters. The use of the normalized difference water index (ndwi) in the delineation of open water features. *International journal of remote sensing*, 17(7):1425–1432, 1996.

S. K. Meerdink, S. J. Hook, D. A. Roberts, and E. A. Abbott. The ecostress spectral library version 1.0. *Remote Sensing of Environment*, 230:111196, 2019.

M. Moshtaghi, E. Knaeps, S. Sterckx, S. Garaba, and D. Meire. Spectral reflectance of marine macroplastics in the vnir and swir measured in a controlled environment. *Scientific Reports*, 11(1):1–12, 2021.

D. Papageorgiou, K. Topouzelis, G. Suaria, S. Aliani, and P. Corradi. Sentinel-2 detection of floating marine litter targets with partial spectral unmixing and spectral comparison with other floating materials (plastic litter project 2021). *Remote Sensing*, 14(23):5997, 2022.

M. Papini. Analysis of the reflectance of polymers in the near-and mid-infrared regions. *Journal of Quantitative Spectroscopy and Radiative Transfer*, 57(2):265–274, 1997.

J. W. Rouse, R. H. Haas, J. A. Schell, D. W. Deering, et al. Monitoring vegetation systems in the great plains with erts. *NASA Spec. Publ*, 351(1):309, 1974.

P. M. Salgado-Hernanz, J. Bauzà, C. Alomar, M. Compa, L. Romero, and S. Deudero. Assessment of marine litter through remote sensing: recent approaches and future goals. *Marine Pollution Bulletin*, 168:112347, 2021.

L. Shen and C. Li. Water body extraction from landsat etm+ imagery using adaboost algorithm. In *2010 18th International Conference on Geoinformatics*, pages 1–4. IEEE, 2010.

P. Tasseron, T. Van Emmerik, J. Peller, L. Schreyers, and L. Biermann. Advancing floating macroplastic detection from space using experimental hyperspectral imagery. *Remote Sensing*, 13(12):2335, 2021.

K. Themistocleous, C. Papoutsa, S. Michaelides, and D. Hadjimitsis. Investigating detection of floating plastic litter from space using sentinel-2 imagery. *Remote Sensing*, 12(16): 2648, 2020.

K. Topouzelis, A. Papakonstantinou, and S. P. Garaba. Detection of floating plastics from satellite and unmanned aerial systems (plastic litter project 2018). *International Journal of Applied Earth Observation and Geoinformation*, 79:175–183, 2019.

K. Topouzelis, D. Papageorgiou, A. Karagaitanakis, A. Papakonstantinou, and M. Arias Ballesteros. Remote sensing of sea surface artificial floating plastic targets with sentinel-2 and unmanned aerial systems (plastic litter project 2019). *Remote Sensing*, 12(12):2013, 2020.

Q. Vanhellemont and K. Ruddick. Acolite for sentinel-2: Aquatic applications of msi imagery. In *Proceedings of the 2016 ESA Living Planet Symposium, Prague, Czech Republic*, pages 9–13, 2016.

C. Wilcox, G. Heathcote, J. Goldberg, R. Gunn, D. Peel, and B. D. Hardesty. Understanding the sources and effects of abandoned, lost, and discarded fishing gear on marine turtles in northern australia. *Conservation biology*, 29(1):198–206, 2015.

H. Xu. Modification of normalised difference water index (ndwi) to enhance open water features in remotely sensed imagery. *International journal of remote sensing*, 27(14): 3025–3033, 2006.

2.4 Mapping Plastic Litter: Integrating a Radiative Transfer Model with the Random Forest machine learning technique

Douglas Galimberti Barbosa[1] *, Bianca Matos de Barros[1] and Cristiano Lima Hackmann[1]

[1]Lab. of Remote Sensing of Coastal and Urban Environments (RESCUE) - Remote Sensing Post-Graduation Program (PPGSR/UFRGS)

* Corresponding author: galimbertidouglas@gmail.com

Abstract

There is a need to monitor plastic pollution on a larger scale. Remote sensing techniques are capable of providing large amounts of data at regular intervals, which enables the analysis of the fate of accumulated plastics in coastal zones. In the present study we investigated the efficacy of different classification approaches of the Random Forest (RF) machine-learning technique for detecting plastic pollution in coastal zones using remote sensing imagery. We applied the Discrete Anisotropic Radiative Transfer (DART) model, generating synthetic images that simulated real-world scenarios of plastic polluted coastal zones to train the RF classifier. Results indicate that integrating spectral indices with multispectral bands significantly enhances plastic detection accuracy, particularly in distinguishing between plastic and water pixels. The Plastic-Water Differentiation Index (PWDI) was the most impactful feature among the spectral bands and indices applied, highlighting the importance of specialized indices tailored to plastics' unique spectral characteristics. PWDI had a feature importance score of over 0.2, followed by the optical bands Green (0.19) and NIR (0.13). Despite challenges posed by imbalanced datasets, approaches combining bands and indices exhibit superior performance in identifying plastic pixels across various polymer types and pixel coverages. This study underscores the advantages of integrating advanced radiative transfer models like DART with machine learning algorithms for accurate plastic pollution monitoring.

Descriptors: waste patches; machine learning; marine ecosystems; macroplastics

INTRODUCTION

Plastic is a flexible material used to produce a wide range of items found in society, ranging from basic containers to electronic parts. It is generally a durable and lightweight material. However, the unsustainable use of plastic results in its direct and passive deposition in natural environments, including the oceans (Jambeck et al. 2015, Meijer et al. 2021). Plastic pollution is considered ubiquitous and negatively affects ecosystems, human health, and economic activities (Andrady 2011, Rahman et al. 2021, Aretoulaki et al. 2021).

Studies that aim to analyse the plastic pollution problem generally apply a combination of visual analysis and *in-situ* material collection, but the data produced might underestimate the actual amount of waste present in the environment (Maximenko et al. 2019). In this context, remote sensing techniques can be a useful complementary tool to monitor plastic pollution on a larger scale (Amézquita Toledo et al. 2017, Garaba & Dierssen 2018, Biermann et al. 2020). But there are limitations concerning the sensors employed, the extensive variety of materials found in marine litter patches, and the aquatic environment itself (Salgado-Hernanz et al. 2021). In addition, raw plastic spectral signatures are different when virgin plastics and plastic litter have their features compared (Garaba & Dierssen 2017, Moshtaghi et al. 2021). Furthermore, current methods struggle to detect wet or submerged plastics (Moshtaghi et al. 2021). For these reasons, it is crucial to produce ground-truth and training data for both the analysis of plastics in different conditions and

Submitted: N/A
Approved: N/A
Editor:

for the improvement of current detection methods.

Currently, the main methodologies of detecting plastic pollution are the employment of (i) spectral indices, (ii) machine learning algorithms, and (iii) controlled laboratory experiments (Biermann et al. 2020, Themistocleous et al. 2020, Wolf et al. 2020, Garaba & Dierssen 2017, Moshtaghi et al. 2021). There are also cases of an integration of multiple methods and also the employment of orbital and aerial sensors to detect plastics (Acuña-Ruz et al. 2018, Garaba & Dierssen 2018, Basu et al. 2021). These approaches employ different sensors, but generally, the Sentinel-2A/2B satellites, equipped with the MultiSpectral Instrument (MSI), are among the most frequently used (Hu 2022). The MSI sensor has 10 to 20 m of spatial resolution and contains spectral bands from the visible (VIS), near infrared (NIR), and short-wave infrared (SWIR), which are adequate to detect floating plastics (Martínez-Vicente et al. 2019, Kikaki et al. 2022, Hu 2022).

The first challenge to detect marine plastic pollution is to distinguish between the spectral shapes of water and plastics. Exposed plastic waste suffers natural weathering effects and gets fragmented into smaller particles overtime, being classified according to its size (Magrini 2012). Current remote sensing techniques only enable the detection of macroplastics ($> 5mm$) (Hu 2022). Waste patches found in coastal waters by Biermann et al. (2020) and Ciappa (2021) were elongated aggregations of floating materials with sizes ranging from 0,2 to 10 km. Therefore, it is crucial to distinguish between plastics and other common targets found in marine waste patches, such as whitecaps, sea weed, algae, driftwood, and timber. Whitecaps are foamy white crests that form when wind blows across the water surface, causing turbulence and wave crashes. Whitecaps are generally bright and are a frequent cause of false positives in plastic detection (Biermann et al. 2020, Dierssen & Garaba 2020).

Another matter is distinguishing between different plastics. Synthetic polymers are created by chemical reactions and are used as the building blocks of plastics. Each plastic has a different polymer composition and exhibits distinct spectral shapes (Garaba & Dierssen 2017, Tasseron et al. 2021). Some plastics, such as polypropylene (PP) and high-density polyethylene (HDPE) are slightly opaque and have higher reflectance values, which facilite the identification of their distinct spectral signatures. PP and HDPE are commonly applied for packaging, textiles, piping, and other consumer goods. Other plastics, like low-density polyethylene (LDPE, plastic bags) and polyethylene terephthalate (PET, plastic bottles), are transparent, thus having lower reflectance values and a more uniform spectral shape.

Within this framework, radiative transfer models can create complex scenery that simulate environmental conditions. The Discrete Anisotropic Radiative Transfer (DART) model was chosen for this study due to its potential to generate remote sensing products with an array of different configurations. It is capable of simulating the electromagnetic spectrum from visible to thermal infrared, as well as including the spectral signatures of objects on the DART scenes (Gastellu-Etchegorry et al. 2012). Consequently, it is possible to examine the spectral signatures of floating matter and the potential to detect plastic litter.

This study's objective is to identify the presence of plastics in coastal zones using remote sensing techniques. We simulated a polluted coastal zone using DART scenes that contained water, plastics, and whitecaps. Plastic targets, composed of LDPE, PET, and PP, were set on the scenes DART scenes. These polymers were chosen due to their abundance when found in natural environments (Schwarz et al. 2019). A series of spectral indices were applied to the DART simulations. Finally, the machine learning algorithm Random Forest was employed to MSI/Sentinel-2 images with confirmed plastic pixels in order to identify the presence of plastics. The input data points, used to train the algorithm were the DART simulated images.

METHODS

Polluted coastal zone simulations

To simulate coastal zones that were polluted by plastics, we constructed scenarios on the Discrete Anisotropic Radiative Transfer (DART) model. This model offers a comprehensive framework for understanding how light interacts with various components such as water, aerosols, and pollutants like plastics. Unlike traditional models, DART's main advantage lies in its capacity to handle anisotropic scattering, making it particularly suitable for scenarios where irregular surface features, such as whitecaps or plastic debris, play a significant role in light interactions (Gastellu-Etchegorry 2008).

Each scene had an area of 1200 x 600 m and featured a combination of water, whitecaps, and square-shaped plastic targets positioned consistently across generated images. To accurately represent the spectral properties of plastic litter, we selected the spectral database produced by Moshtaghi et al. (2021), comprising plastics collected *in-situ*, which depicts the weathering experienced in natural environments. This study measured the spectra of plastics with a spectroradiometer in controlled laboratory experiments. The chosen polymers included Low-Density Polyethylene (LDPE), Polyethylene Terephthalate (PET), and

Polypropylene (PP). LDPE and PET were simulated in dry conditions. PP was represented in white and orange colors, each exhibiting wet and submerged states at depths of 2 cm and 5 cm. The water's spectral signature, already present in the DART spectral library, represented clean oceanic water (Meerdink et al. 2019).

The spectral signature of whitecaps were simulated using a third-degree polynomial (Equation 1) that accounts for the water absorption coefficient:

$$\begin{aligned} R_f &= 0.47x^3 - 1.62x^2 + 8.66x + 31.81 \\ x &= \log(\alpha_w) \\ \alpha_w(m^{-1}) &= \text{Absorption coefficient of water.} \end{aligned} \tag{1}$$

This spectral signature is a result of the study conducted by Dierssen (2019), which stated that this spectral signature is an adequate representation of the mean value of whitecaps measured in aquatic environments.

For our simulations, we selected the MultiSpectral Instrument (MSI) aboard the Sentinel-2A and 2B satellite constellation. We included the optical bands specified on table 1. The Coastal ($B1$), Water Vapor ($B9$), and SWIR Cirrus ($B10$) bands were not considered in this study.

Table 1. MSI/Sentinel-2 specifications. Bands in the color grey were not included in the DART simulations.

Band	Name	Central λ (nm)	Spatial res. (m)
B1	Coastal	443	60
B2	Blue	492	10
B3	Green	560	10
B4	Red	665	10
B5	$RedEdge_1$	704	20
B6	$RedEdge_2$	741	20
B7	$RedEdge_3$	783	20
B8	NIR	833	10
B8a	Narrow NIR	865	20
B9	Water Vapor	945	60
B10	SWIR Cirrus	1374	60
B11	$SWIR_1$	1614	20
B12	$SWIR_2$	2202	20

These sensor configurations were integrated into the DART model to ensure accurate representation and analysis of the simulated scenes. The DART simulations comprised two main groups. The first group focused on varying the plastic-to-pixel proportions relative to the Sentinel-2 pixel. Plastic targets were set at different proportions, including 40%, 60%, 80%, and 100% of the pixel area. The second group explored different whitecap-to-plastic proportions within the scenes. Whitecaps were varied from 100%, 60%, 40% to 20%, allowing for analysis of how whitecaps influence the detection and characterization of plastic pollution in coastal zones.

Sentinel-2 images

In order to acquire MSI/Sentinel-2 images with confirmed presence of plastic pixels, we employed the products of the studies developed by Topouzelis et al. (2020) and Papageorgiou et al. (2022), which are results of the Plastic Litter Project (PLP), developed in Greece. In this project, targets filled with different plastic polymers were built and anchored at sea in order to fill 100% of the MSI pixel (10 m). There were targets composed on LDPE and PET on PLP 2019. Finally, there were LDPE, PET, HDPE-mesh, and wooden targets on PLP 2021. In total, 10 level-1C images spanning from 2019 to 2021 were freely acquired from the United States Geological Service (USGS) and the Copernicus Access Hub. Throughout this work, we refer to this set of images as "USGS images". After visual inspection and cross-referencing with geolocation data, 103 plastic pixels were annotated.

Image processing

We standardized the spatial resolution of the DART and the USGS images to 10 m by applying the Resampling[1] function in a Python script. We opted for the bilinear interpolation mode over the near and cubic modes because of its reduced amplitude when compared to the other two. This choice resulted in a more accurate alignment with the distribution of the USGS images.

Afterwards, the USGS level-1C products underwent atmospheric correction by using the Atmospherical Correction for OLI Lite (ACOLITE) algorithm, using the Dark Spectrum Fitting (DSF) mode. This mode leverages dark pixel spectra to estimate the inherent optical properties of water, being considered adequate to the application in aquatic environments (Vanhellemont & Ruddick 2016).

Then, the USGS images were cropped, using the Sentinel Application Platform (SNAP - version 8.0), so that we could focus only on the specific areas of interest for this study.

[1] Source and more details: http://tinyurl.com/resampling

The DART and USGS images had their spatial and spectral data integrated into a Python script to facilitate their analysis and classification. The simulated image pixels were labeled with a rule of 100% water coverage being considered "Water" and any percentage of plastics was considered "Plastic". The USGS images, however, were classed according to partial (less than 100%) and full (100%) of plastic coverage; there was also the labeling of the "Coast" and "Wood" pixels.

Spectral indices

A series of spectral indices were applied to the DART and USGS images, aiming to test their potential to detect plastics (Table 2). All details regarding band math and original sources can be verified in the Appendix (Page 8). The Floating Debris Index (FDI), developed by Biermann et al. (2020), was succesfully applied to detect floating plastic pixels on waste patches along different coastal zones. The FDI is applied in conjunction with the Normalized Difference Vegetation Index (NDVI) to detect floating matter and separate the vegetation from plastics (Biermann et al. 2020).

The Plastic Index (PI) and the Reversed Normalized Difference Vegetation Index (RNDVI), were both developed by Themistocleous et al. (2020). According to their findings, it was shown that the combined use of PI and RNDVI was able to detect plastic bottle (PET) targets constructed in the study and set at sea in MSI/Sentinel-2 images. The study also tested the effectiveness of water extraction (AWEI, WRI, NDWI, MNDWI) and vegetation detection (NDVI, SR) indices for the identification of plastic litter.

Table 2. Spectral indices applied in this study.

Spectral Index	Application
AWEI	Water detection
WRI	
NDWI	
MNDWI	
NDVI	Vegetation detection
RNDVI	
SR	
PWDI	Plastic detection
FDI	
PI	

The Plastic-Water Differentiation Index (PWDI) was developed by Barbosa et al. (2024). It leverages the unique features of plastics in the NIR ($B8$) and RedEdge_3 ($B6$) spectra, enabling the differentiation between pure water and water with the presence of floating matter according to the study's findings. This spectral index was created based on the characteristic absorption lines and overall spectral behavior of plastics, which is a result of their molecular composition. Furthermore, the PWDI had the most prominent separation between water and plastic pixels in the DART simulated images.

Supervised classification algorithm

In order to detect plastics in the USGS images, we selected the Random Forest (RF) algorithm. This is a popular machine learning algorithm widely used in remote sensing applications for image classification tasks. It is known for its ability to handle high-dimensional data, deal with noisy data, and provide estimates of feature importance (Ghose et al. 2010). This algorithm operates by constructing a multitude of decision trees during the training phase. During prediction, each tree votes for a class, and the class with the most votes (mode) is assigned as the final prediction. It was chosen for this study because it generates an importance score for every feature utilized in the classification, indicating which one was more impactful for the decision trees.

We employed the RF algorithm by training it on simulated data generated using the DART model. This training data included LDPE, PET, and PP plastic pixels at different pixel covereages, allowing the algorithm to learn the spectral signatures associated with plastic pollution. The selected maximum depth for trees was set to 3 levels. This value yielded the highest accuracy in classifying the simulated data according to de Barros et al. (2023). Feature importance calculations for each dataset were visually represented through graphical means. By leveraging the capabilities of the MSI/Sentinel-2 optical bands, we tested if the algorithm could effectively distinguish between the "Plastic" and "Water" classes. Three distinct approaches were explored to check for their effectiveness: only MSI/Sentinel-2 bands (Table 1), only spectral indices (Table 2), both bands and indices. They will be referred to in this study as Classification Approach (CA) 1, 2, and 3. There were 100 iterations of the algorithm in order to test its consistency across all metrics.

RESULTS AND DISCUSSION

The labeling of the DART and USGS images revealed an imbalance between all classes when compared with plastics, which is to be expected when observing coastal zones with floating matter and possible plastic pixels. As seen in Figure 1, plastic makes up 1.75% of the total pixels in the DART images, whereas in the

USGS images it represents 2.59% and 4.21% for the years of 2019 and 2021 respectively.

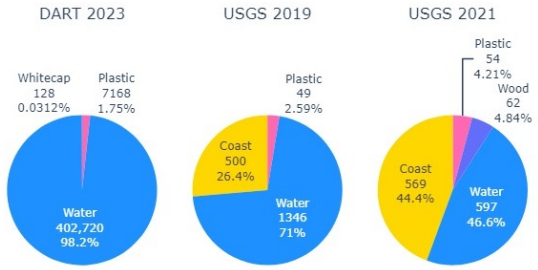

Figure 1. Class distribution of all pixels from the DART and USGS images.

The evaluation metrics generated by the Random Forest algorithm are detailed in table 3 in order to see how it performed on the three employed approaches.

Regarding the overall accuracy (OA), the Classification Approach (CA) 1 and CA3 had similar performances (0.95 and 0.88). This means that they were able to correctly label an overall majority of pixels across all images. However, this metric does not address the imbalances on the dataset. Comparatively, CA2 only managed to achieve a value of 0.05, which indicates it only classified a very small percentage of pixels correctly. In a case-by-case analysis of the generated classification maps, a majority of pixels were classified as “Plastic” by CA2.

Table 3. Evaluation metrics attributed to each classification approach that was employed.

Metric	CA1	CA2	CA3
Overall accuracy	0.953	0.053	0.884
Balanced accuracy	0.536	0.501	0.599
F1 macro	0.555	0.05	0.595
F1 weighted	0.933	0.009	0.893
Fbeta macro	0.615	0.037	0.638
Fbeta weighted	0.927	0.014	0.91
Precision macro	0.909	0.525	0.701
Precision weighted	0.949	0.951	0.934
Recall macro	0.536	0.501	0.599
Recall weighted	0.953	0.053	0.884

The balanced accuracy (BA) is a crucial metric for the analysing this dataset. It calculates the average accuracy across all classes, ensuring that each class contributes equally to the final score regardless of its size. It is particularly useful when dealing with imbalanced datasets where one class dominates the others. When observing CA1 and CA3, they are similar, but there is a noticeable improvement on the latter (0.53 compared to 0.59). This suggests that CA3 is better at correctly classifying pixels across different classes, not just the majority class. Interestingly, CA2, which had a very low OA, had a similar value to the previous two (0.5). This demonstrates a fair performance of this approach across all classes. Nevertheless, CA2 shows more overall false positives and negatives.

The increase in the F1 macro score for CA3 suggests improved performance across all classes. However, the slight decrease in the F1 weighted score indicates that CA3 prioritizes performance on minority classes at the expense of the majority class. The two F1 scores of CA2 are drastically lower compared to the other two. This suggests that it is not effectively balancing precision and recall. In other words, it is evenly misclassifying across classes at a high rate (as suggested by the BA metric).

The macro precision for CA1 is substantially higher than the other approaches, indicating that when it predicts a class, it’s more likely correct. However, it has a lower macro recall score than CA3, suggesting that it may be too conservative, missing a lot of actual positives. CA3 is better at identifying all classes of plastic pixels (Table 4. This is important in the case of missing an actual positive (a plastic pixel) which could be more detrimental than incorrectly labeling a non-plastic pixel. The weighted recall follows the trend of OA.

CA1 is more accurate overall and the best at predicting the majority class. However, due to the high precision and lower recall, it misses many actual positives. When observing Table 4, it only managed to correctly detect 13.9% of the total HDPE pixels and missed all LDPE and PET pixels. CA3, while less accurate overall, has a better BA, macro F1, and macro recall, demonstrating that it is more effective at detecting plastic pixels across all polymer types. It was able to detect 47% of HDPE pixels. This comes at the cost of precision, meaning that it may incorrectly label more non-plastic pixels as Plastic. Finally, CA2 seems to be ineffective for this task, since it has very poor accuracy in general. Despite it having a reasonably high BA (0.5) and consistently detecting plastic pixels, the approach’s utility is questionable since it incorrectly classified the vast majority of the Water class as Plastic.

The plastic-to-pixel coverages in the USGS images revealed that it was easier to detect plastics at higher values. At 100% plastic coverage, the CA3 approach was able to correctly detect 81% of pixels, while CA1 was able to detect 40.9%. Whereas, in the <25% range, CA3 was able to detect 6.4% of pixels correctly, while CA1 detected 0%.

In relation to polymers, identifying LDPE and PET

Table 4. Plastic pixels that were correctly labeled in the USGS images by the CA1 and CA3 approaches.

Polymer	Pixels	Bands				Both			
		Mean hits (%)	StD hits	Min hits (%)	Max hits (%)	Mean hits (%)	StD hits	Min hits (%)	Max hits (%)
LDPE	20	0.0 (0.0 %)	0	0 (0.0 %)	0 (0.0 %)	1.16 (5.8 %)	2.784	0 (0.0 %)	19 (95.0 %)
PET	25	0.0 (0.0 %)	0	0 (0.0 %)	0 (0.0 %)	1.91 (7.6 %)	3.72	0 (0.0 %)	23 (92.0 %)
LDPE and PET	4	0.0 (0.0 %)	0	0 (0.0 %)	0 (0.0 %)	0.61 (15.2 %)	1.043	0 (0.0 %)	4 (100.0 %)
HDPE	54	7.51 (13.9 %)	2.721	1 (1.9 %)	15 (27.8 %)	25.4 (47.0 %)	9.294	17 (31.5 %)	54 (100.0 %)

targets seems to be more challenging than detecting HDPE. This is because of the semi-transparent quality of these polymers, which results in an overall decrease in their measure reflectance, as well as spectral shapes with less distinct peaks and valleys. They are also more prone to absorbing water than HDPE, which increases the strong light absorption effect caused by this (Hamilton 1967). On the other hand, HDPE is a more opaque polymer, which increases the intensity of the scattered and reflected light (Papini 1997). Incorporating HDPE targets in the DART simulations might have a positive impact in the detection ratio of this polymer in the USGS images.

Overall, the inclusion of spectral indices alongside optical MSI/Sentinel-2 bands in the CA3 approach offers a more equitable classification across different classes, at the cost of some OA and precision. If the goal is to minimize false negatives (missing plastic pixels), CA3 is better. If the goal is to ensure a high confidence in the positive predictions made (precision), CA1 might be preferred.

Cross-study comparison

Comparing studies on plastic detection in coastal zones using remote sensing and machine learning entails considering various factors like sensor types, classification algorithms, feature sets, and environmental conditions. In the case of the study developed by Biermann et al. (2020), it reportedly had 86% accuracy rate by using the FDI, NDVI, and the Naïve-Bayes classifier to detect plastics across different coastal zones. It dealt with a more complex and heterogenous environment, in which sargassum and driftwood was associated with plastic litter. But, it was proven that the FDI was not capable of detecting submerged plastic debris, according to Moshtaghi et al. (2021).

Themistocleous et al. (2020) developed the PI and RNDVI to detect targets constructed with PET bottles and polyvinyl chloride (PVC) frames. It was succesful in the detection of both the PET targets and plastic litter in a coastal zone with the presence of floating fish farms. It was able to detect plastic fishing collars of 0.5-1.10 m in diamater. It combined both MSI/Sentinel-2 imagery with unmanned aerial vehicles (UAVs) to detect plastics. This is an example of a study that used more than one kind of sensor to detect plastics.

Barbosa et al. (2024) made use of experiments with the application of the K-means algorithm with different data points. Nevertheless, gauging the extent of the PWDI's impact on the algorithm proved challenging. With the application of RF, which assigns distinct scores to each feature, this task was made much simpler. Our updated dataset exhibits a marked advancement from prior research, unequivocally demonstrating the positive impact of PWDI.

The work developed by Garaba & Harmel (2022) employed the 6SV radiative transfer model to simulate the top-of-atmosphere spectral signature of plastics. It's findings revealed that plastics submerged in the top 1 m of the water column were detectable by the sensors of the WorldView-3, Sentinel-2, and Sentinel-3 satellites. Both this study and the results presented by Garaba & Harmel (2022) also employed a radiative transfer model and the detection of plastic litter. However, in the latter there was a focus on the spectral signatures of plastics under different water clarity and depth conditions. Our study demonstrated the performance of the Random Forest algorithm, which was trained applying the data generated by the DART model, in correctly identifying plastics on Sentinel-2 images.

Performance wise, our results are comparable to some other studies. Acuña-Ruz et al. (2018) employed RF, Linear Discriminant Analysis (LDA), and Support Vector Machine (SVM) algorithms to detect plastic litter, more specifically polystyrene boxes on a seashore. They managed to achieve >75% accuracy using RF and LDA, and a highest accuracy score of 90% using SVM. Basu et al. (2021) combined unsupervised (K-means and Fuzzy C-means) and supervised (Support Vector Regression and Semi-supervised Fuzzy C-means) algorithms to detect plastics in the Sentinel-2 images featured in the PLP and the study developed by Themistocleous et al. (2020). It achieved very high accuracies, up to 98.4%, but did not manage to detect plastic pixels efficiently, similar to the Bands approach applied in our study.

Feature importance

The RF algorithm provides a measure of the contribution of each feature to the model's predictive perfor-

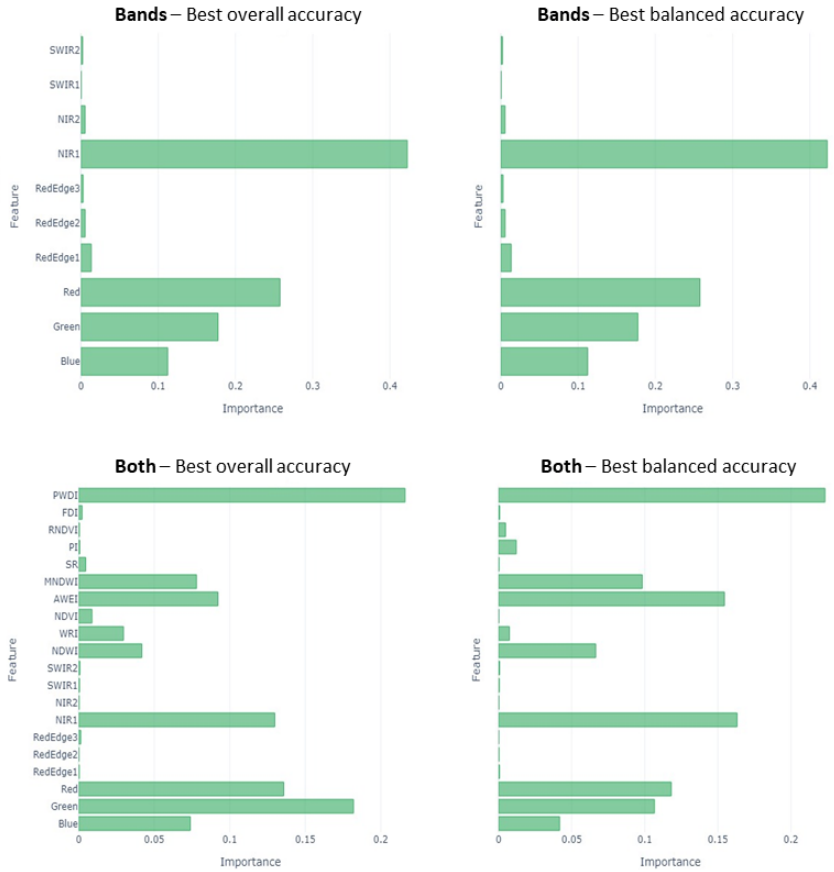

Figure 2. Feature importance scores generated by the Random Forest algorithm.

mance. The Gini impurity[2] is used to measure the quality of a split in the decision trees. It calculates how much each feature reduces the weighted impurity across all trees in the forest. The feature importances pertaining to the Bands and Both approaches can be observed in Figure 2.

The most impactful feature in the Bands approach was NIR ($B8$), while the least impactful was $SWIR_1$ ($B11$). Reportedly, $B8$ is a very important optical band for plastic detection (Tasseron et al. 2021, Moshtaghi et al. 2021). According to Biermann et al. (2020), plastics have reflectance peak in this spectral range and water has a distinct absorption line. This band is also extensively used in factorial settings to identify plastic particles for recycling (Huth-Fehre et al. 1995). As for $B11$, Hu (2022) has stated that around this spectral range, the already low reflectance values can be reduced by 1 million times if the floating matter is just 1 cm below the water surface. So, it is justified that both $B11$ and $B12$ did not have a good performance.

The feature importances for the approach that applied both bands and indices demonstrated that the PWDI had the most impact across all features. The PWDI leverages the contrast between the NIR ($B8$) reflectance peak and $RedEdge_3$ ($B7$) absorption line, which was also demonstrated by the DART simulations. This agrees with the findings from Barbosa et al. (2024), which demonstrated the greater separability of water and plastic pixels by the PWDI when compared to the other spectral indices. The second and third most impactful spectral indices were the AWEI and MNDWI. This underscores the importance of water extraction indices for plastic detection. On the other hand, the vegetation monitoring indices did not have much impact in this case. Testing on environments that contain floating vegetation, as well as the inclusion of vegetation on the DART simulations, are necessary to further test their capabilities.

Concerning the bands from the VIS spectra ($B2$,$B3$,$B4$), they were, overall, some of the most important features as well. They are very important bands for detecting water pixels (Nguyen 2012). All the water spectral indices applied in the present study contain at least one VIS band. Moshtaghi et al. (2021) stated that, depending on the plastic's color, each band from VIS can be a defining factor in order to detect it correctly.

[2]Description and details about the Random Forest algorithm: https://tinyurl.com/rndmforest

CONCLUSION

We demonstrated in our study that the Discrete Anisotropic Radiative Transfer (DART) model advanced our understanding of plastic pollution in coastal zones. By simulating the interaction of light with various types of plastics and environmental conditions, the DART model provides crucial insights into the spectral signatures of plastics, enabling the development of the Plastic-Water Differentiation Index (PWDI). In this study, we leveraged the capabilities of the DART model to generate synthetic images that simulate real-world scenarios, allowing us to assess the performance of different classification approaches in identifying plastic pixels in satellite imagery. In the future, we expect to enhance the realism portrayed by the DART simulations by adding vegetation and wood spectral signatures, in order to represent the recurring association of sargassum and driftwood with plastic litter.

Our findings highlight the importance of adopting a comprehensive approach that combines both optical bands and spectral indices for plastic detection. The inclusion of spectral indices alongside traditional multispectral bands significantly enhances the classification performance, particularly in distinguishing between plastic and water pixels. The feature importance analysis conducted as part of our study provides valuable insights into the key factors influencing the classification of plastic pixels. Among the spectral indices evaluated, the PWDI stood out as the most impactful feature, demonstrating its effectiveness in differentiating between plastic and water pixels. This underscores the significance of developing specialized indices tailored to the unique spectral characteristics of plastic litter. NIR ($B8$), emerged as a crucial feature for plastic detection, owing to the distinct reflectance peak exhibited by plastics in this spectral range. Additionally, water extraction indices such as the AWEI and MNDWI showed significant impact, highlighting the importance of leveraging spectral contrast between plastics and surrounding water bodies for accurate classification.

Furthermore, our study emphasizes the challenges associated with imbalanced datasets, where the presence of plastics constitutes only a small fraction of the total pixels. While traditional classification approaches based solely on optical bands achieve high overall accuracy, they may struggle to accurately detect plastic pixels, especially those belonging to minority classes such as LDPE and PET. Our testing of the approach that integrates spectral indices exhibited better performance in correctly detecting plastic pixels across different polymer types and pixel coverages, albeit at the cost of slightly lower overall accuracy and precision.

In conclusion, our study demonstrates that the integration of radiative transfer models, such as DART, with machine learning algorithms enhances plastic detection in coastal zones. By harnessing the spectral signatures of plastics and developing specialized indices tailored to their unique characteristics, we can improve the accuracy and effectiveness of remote sensing plastic pollution monitoring techniques.

APPENDIX

Band equations of spectral indices applied in this study (expressed in terms of the MSI/Sentinel-2 bands)

Automated Water Extraction Index (Feyisa et al. 2014)

$$AWEI = 4 * (B3 - B12) - (0.25 * B8 + 2.75 * B11)$$

Water Ratio Index (Shen & Li 2010)

$$WRI = \frac{B3+B4}{B8+B12}$$

Normalized Difference Water Index (McFeeters 1996)

$$NDWI = \frac{B3-B8}{B3+B8}$$

Modified Normalized Difference Water Index (Xu 2006)

$$MNDWI = \frac{B3-B12}{B4+B12}$$

Normalized Difference Vegetation Index (Rouse et al. 1974)

$$NDVI = \frac{B8-B4}{B8+B4}$$

Reversed Normalized Difference Vegetation Index (Themistocleous et al. 2020)

$$RNDVI = \frac{B4-B8}{B4+B8}$$

Simple Ratio (Jordan 1969)

$$SR = \frac{B8}{B4}$$

Plastic Water Differentation Index

$$PWDI = \frac{B8-B6}{B8+B6}$$

Floating Debris Index (Biermann et al. 2020)

$$FDI = R_{rs,B8} - R'_{rs,B8}$$
$$R'_{rs,B8} = R_{rs,B6} + (R_{rs,B11} - R_{rs,B6}) \times \frac{(\lambda_{B8}-\lambda_{B4})}{(\lambda_{B11}-\lambda_{B4})} \times 10$$

Plastic Index (Themistocleous et al. 2020)

$$PI = \frac{B8}{B8+B4}$$

REFERENCES

ACUÑA-RUZ, T., URIBE, D., TAYLOR, R., AMÉZQUITA, L., GUZMÁN, M. C., MERRILL, J., MARTÍNEZ, P., VOISIN, L. & MATTAR, C. 2018. Anthropogenic marine debris over beaches: Spectral characterization for remote sensing applications, *Remote Sensing of Environment* **217**: 309–322.

AMÉZQUITA TOLEDO, L. P. ET AL. 2017. Elaboración de una propuesta para la gestión integral de residuos antropogénicos costeros en el archipiélado de chiloé, chile.

ANDRADY, A. L. 2011. Microplastics in the marine environment, *Marine pollution bulletin* **62**(8): 1596–1605.

ARETOULAKI, E., PONIS, S., PLAKAS, G., AGALIANOS, K. ET AL. 2021. Marine plastic littering: A review of socio economic impacts, *J. Sustain. Sci. Manag* **16**(3): 277–301.

BARBOSA, D. G., DE BARROS, B. M. & HACKMANN, C. L. 2024. Development of a novel plastic-water differentiation index for detecting plastic debris in sentinel-2 imagery, *Unpublished manuscript* .

BASU, B., SANNIGRAHI, S., SARKAR BASU, A. & PILLA, F. 2021. Development of novel classification algorithms for detection of floating plastic debris in coastal waterbodies using multispectral sentinel-2 remote sensing imagery, *Remote Sensing* **13**(8): 1598.

BIERMANN, L., CLEWLEY, D., MARTINEZ-VICENTE, V. & TOPOUZELIS, K. 2020. Finding plastic patches in coastal waters using optical satellite data, *Scientific reports* **10**(1): 1–10.

CIAPPA, A. C. 2021. Marine plastic litter detection offshore hawai'i by sentinel-2, *Marine Pollution Bulletin* **168**: 112457.

DE BARROS, B. M., BARBOSA, D. G. & HACKMANN, C. L. 2023. Spectral analysis of marine debris in simulated and observed sentinel-2/msi images using unsupervised classification, *arXiv preprint arXiv:2306.15008* .

DIERSSEN, H. M. 2019. Hyperspectral measurements, parameterizations, and atmospheric correction of whitecaps and foam from visible to shortwave infrared for ocean color remote sensing, *Frontiers in Earth Science* **7**: 14.

DIERSSEN, H. M. & GARABA, S. P. 2020. Bright oceans: Spectral differentiation of whitecaps, sea ice, plastics, and other flotsam, *Recent Advances in the Study of Oceanic Whitecaps*, Springer, pp. 197–208.

FEYISA, G. L., MEILBY, H., FENSHOLT, R. & PROUD, S. R. 2014. Automated water extraction index: A new technique for surface water mapping using landsat imagery, *Remote sensing of environment* **140**: 23–35.

GARABA, S. & DIERSSEN, H. 2017. Spectral reference library of 11 types of virgin plastic pellets common in marine plastic debris, *Data set available on-line [http://ecosis. org] from the Ecological Spectral Information System (EcoSIS). http://dx. doi. org/10* **21232**: C27H34.

GARABA, S. P. & DIERSSEN, H. M. 2018. An airborne remote sensing case study of synthetic hydrocarbon detection using short wave infrared absorption features identified from marine-harvested macro-and microplastics, *Remote sensing of environment* **205**: 224–235.

GARABA, S. P. & HARMEL, T. 2022. Top-of-atmosphere hyper and multispectral signatures of submerged plastic litter with changing water clarity and depth, *Optics Express* **30**(10): 16553–16571.

GASTELLU-ETCHEGORRY, J.-P. 2008. 3d modeling of satellite spectral images, radiation budget and energy budget of urban landscapes, *Meteorology and atmospheric physics* **102**(3): 187–207.

GASTELLU-ETCHEGORRY, J.-P., GRAU, E. & LAURET, N. 2012. Dart: A 3d model for remote sensing images and radiative budget of earth surfaces, *Modeling and simulation in Engineering* pp. ISBN–978.

GHOSE, M., PRADHAN, R. & GHOSE, S. S. 2010. Decision tree classification of remotely sensed satellite data using spectral separability matrix, *International Journal of Advanced Computer Science and Applications* **1**(5).

HAMILTON, R. 1967. Water vapor permeability of polyethylene and other plastic materials, *Bell System Technical Journal* **46**(2): 391–415.

HU, C. 2022. Remote detection of marine debris using sentinel-2 imagery: A cautious note on spectral interpretations, *Marine Pollution Bulletin* **183**: 114082.

HUTH-FEHRE, T., FELDHOFF, R., KANTIMM, T., QUICK, L., WINTER, F., CAMMANN, K., VAN DEN BROEK, W., WIENKE, D., MELSSEN, W. & BUYDENS, L. 1995. Nir-remote sensing and artificial neural networks for rapid identification of post consumer plastics, *Journal of Molecular Structure* **348**: 143–146.

JAMBECK, J. R., GEYER, R., WILCOX, C., SIEGLER, T. R., PERRYMAN, M., ANDRADY, A., NARAYAN, R. & LAW, K. L. 2015. Plastic waste inputs from land into the ocean, *Science* **347**(6223): 768–771.

JORDAN, C. F. 1969. Derivation of leaf-area index from quality of light on the forest floor, *Ecology* **50**(4): 663–666.

KIKAKI, K., KAKOGEORGIOU, I., MIKELI, P., RAITSOS, D. E. & KARANTZALOS, K. 2022. Marida: A benchmark for marine debris detection from sentinel-2 remote sensing data, *PloS one* **17**(1): e0262247.

MAGRINI, A. 2012. *Impactos ambientais causados pelos plásticos: uma discussão abrangente sobre os mitos e os dados científicos*, Editora E-papers.

MARTÍNEZ-VICENTE, V., CLARK, J. R., CORRADI, P., ALIANI, S., ARIAS, M., BOCHOW, M., BONNERY, G., COLE, M., CÓZAR, A., DONNELLY, R. ET AL. 2019. Measuring marine plastic debris from space: Initial assessment of observation requirements, *Remote Sensing* **11**(20): 2443.

MAXIMENKO, N., CORRADI, P., LAW, K. L., VAN SEBILLE, E., GARABA, S. P., LAMPITT, R. S., GALGANI, F., MARTINEZ-VICENTE, V., GODDIJN-MURPHY, L., VEIGA, J. M. ET AL. 2019. Toward the integrated marine debris observing system, *Frontiers in marine science* **6**.

MCFEETERS, S. K. 1996. The use of the normalized difference water index (ndwi) in the delineation of open water features, *International journal of remote sensing* **17**(7): 1425–1432.

MEERDINK, S. K., HOOK, S. J., ROBERTS, D. A. & ABBOTT, E. A. 2019. The ecostress spectral library version 1.0, *Remote Sensing of Environment* **230**: 111196.

MEIJER, L. J., VAN EMMERIK, T., VAN DER ENT, R., SCHMIDT, C. & LEBRETON, L. 2021. More than 1000 rivers account for 80% of global riverine plastic emissions into the ocean, *Science Advances* **7**(18): eaaz5803.

MOSHTAGHI, M., KNAEPS, E., STERCKX, S., GARABA, S. & MEIRE, D. 2021. Spectral reflectance of marine macroplastics in the vnir and swir measured in a controlled environment, *Scientific Reports* **11**(1): 1–12.

NGUYEN, D. 2012. Water body extraction from multi spectral image by spectral pattern analysis, *The International Archives of the Photogrammetry, Remote Sensing and Spatial Information Sciences* **39**: 181–186.

PAPAGEORGIOU, D., TOPOUZELIS, K., SUARIA, G., ALIANI, S. & CORRADI, P. 2022. Sentinel-2 detection of floating marine litter targets with partial spectral unmixing and spectral comparison with other floating materials (plastic litter project 2021), *Remote Sensing* **14**(23): 5997.

PAPINI, M. 1997. Analysis of the reflectance of polymers in the near-and mid-infrared regions, *Journal of Quantitative Spectroscopy and Radiative Transfer* **57**(2): 265–274.

RAHMAN, A., SARKAR, A., YADAV, O. P., ACHARI, G. & SLOBODNIK, J. 2021. Potential human health risks due to environmental exposure to nano-and microplastics and knowledge gaps: A scoping review, *Science of the Total Environment* **757**: 143872.

ROUSE, J. W., HAAS, R. H., SCHELL, J. A., DEERING, D. W. ET AL. 1974. Monitoring vegetation systems in the great plains with erts, *NASA Spec. Publ* **351**(1): 309.

SALGADO-HERNANZ, P. M., BAUZÀ, J., ALOMAR, C., COMPA, M., ROMERO, L. & DEUDERO, S. 2021. Assessment of marine litter through remote sensing: recent approaches and future goals, *Marine Pollution Bulletin* **168**: 112347.

SCHWARZ, A. E., LIGTHART, T. N., BOUKRIS, E. & VAN HARMELEN, T. 2019. Sources, transport, and accumulation of different types of plastic litter in aquatic environments: a review study, *Marine pollution bulletin* **143**: 92–100.

SHEN, L. & LI, C. 2010. Water body extraction from landsat etm+ imagery using adaboost algorithm, *2010 18th International Conference on Geoinformatics*, IEEE, pp. 1–4.

TASSERON, P., VAN EMMERIK, T., PELLER, J., SCHREYERS, L. & BIERMANN, L. 2021. Advancing floating macroplastic detection from space using experimental hyperspectral imagery, *Remote Sensing* **13**(12): 2335.

THEMISTOCLEOUS, K., PAPOUTSA, C., MICHAELIDES, S. & HADJIMITSIS, D. 2020. Investigating detection of floating plastic litter from space using sentinel-2 imagery, *Remote Sensing* **12**(16): 2648.

TOPOUZELIS, K., PAPAGEORGIOU, D., KARAGAITANAKIS, A., PAPAKONSTANTINOU, A. & ARIAS BALLESTEROS, M. 2020. Remote sensing of sea surface artificial floating plastic targets with sentinel-2 and unmanned aerial systems (plastic litter project 2019), *Remote Sensing* **12**(12): 2013.

VANHELLEMONT, Q. & RUDDICK, K. 2016. Acolite for sentinel-2: Aquatic applications of msi imagery, *Proceedings of the 2016 ESA Living Planet Symposium, Prague, Czech Republic*, pp. 9–13.

WOLF, M., VAN DEN BERG, K., GARABA, S. P., GNANN, N., SATTLER, K., STAHL, F. & ZIELINSKI, O. 2020. Machine learning for aquatic plastic litter detection, classification and quantification (aplastic-q), *Environmental Research Letters* **15**(11): 114042.

XU, H. 2006. Modification of normalised difference water index (ndwi) to enhance open water features in remotely sensed imagery, *International journal of remote sensing* **27**(14): 3025–3033.

3 CONCLUSÕES

A análise das características espectrais dos plásticos e outros alvos comuns aos ambientes marinhos, em imagens de sensoriamento remoto reais e simuladas, forneceu conhecimentos indispensáveis sobre a efetividade e as limitações das técnicas de detecção atuais. Foi demonstrado que o modelo DART é capaz de gerar assinaturas espectrais que são de grande valia para entender o comportamento dos polímeros em zonas costeiras, assim como treinar algoritmos de aprendizado de máquina para classificação de imagens. O controle da composição das cenas, onde é possível mudar os tipos de polímeros, seus tamanhos e adicionar outros alvos é um grande diferencial para estudos desta problemática. Em trabalhos futuros, a incorporação de vegetação e madeira pode aumentar o realismo das cenas construídas no modelo DART.

Através da análise das imagens geradas pelo modelo DART e da estrutura molecular dos polímeros foi possível desenvolver o Plastic-Water Differentiation Index (PWDI). O índice radiométrico PWDI demonstrou a separação entre plástico e água nas imagens simuladas pelo modelo DART. Sua incorporação no método de clusterização *K-means* demonstrou aspectos positivos relacionados à utilização de índices em conjunto com bandas espectrais para a detecção dos plásticos. O algoritmo foi capaz de agrupar polipropileno nas imagens simuladas, denotando a importância deste polímero. Os resultados provenientes da aplicação nas imagens MSI/Sentinel-2 com presença confirmada de plásticos demonstraram que, com a incorporação do PWDI, foi possível a diferenciação entre água pura e água com presença de matéria flutuante (plásticos e madeira). Esta diferenciação ficou mais clara também nas imagens de 2021, devido aos alvos de polietileno de alta densidade (HDPE). Por fim, há uma hipótese de que 40% de cobertura do pixel MSI por plásticos seja um limite para sua detecção.

Os resultados da aplicação da técnica de aprendizado de máquina *Random Forest* (RF) revelaram a importância de integrar índices radiométricos em conjunto com bandas espectrais para detectar plásticos em ambientes marinhos. A distinção entre pixels de água e plásticos foi aumentada significativamente através desta conjunção. A utilização da abordagem com uso exclusivo de bandas espectrais revelou uma alta acurácia geral, porém, com altas taxas de falsos negativos.

Ademais, a abordagem com aplicação apenas de índices radiométricos se mostrou ineficiente de modo geral. De acordo com o cálculo de importância de todas as *features* empregadas pelo algoritmo RF, o PWDI possuiu a pontuação mais alta, e portanto foi o índice radiométrico mais impactante para as decisões do classificador. Outras *features* consideravelmente impactantes foram a banda espectral NIR e o Automated Water-Extraction Index (AWEI).

Comparativamente, os resultados obtidos com o algoritmo RF destacam-se em relação ao método *K-means* aplicado nos dois estudos. Enquanto o *K-means* foi eficaz na clusterização das imagens, sua capacidade de fornecer uma avaliação quantitativa do impacto de diferentes abordagens e características foi limitada. Por outro lado, o RF permitiu uma análise mais detalhada e precisa. Foram geradas pontuações para cada abordagem, assim como para a importância de todas as bandas espectrais e índices utilizados. Essa abordagem quantitativa do RF proporcionou uma compreensão mais profunda do desempenho das diferentes estratégias de detecção de plástico, permitindo uma avaliação mais robusta do impacto do PWDI e de outros índices radiométricos na precisão da detecção. Assim, o RF emergiu como uma ferramenta superior para a classificação de imagens de sensoriamento remoto em relação ao *K-means*, oferecendo *insights* mais claros e precisos para o monitoramento da poluição por plásticos em zonas costeiras.

Este trabalho foi realizado junto ao grupo de pesquisa *Remote Sensing of Coastal and Urban Environments* (RESCUE). Previamente, o estudo desenvolvido por De Barros (2023) também demonstrou a utilização do modelo DART e da técnica de clusterização *K-means* para analisar a assinatura espectral de polímeros e detectar plásticos em imagens MSI/Sentinel-2. As maiores coberturas de plásticos no pixel também foram associadas a uma maior taxa de detecção correta da poluição. No entanto, comparativamente, os principais avanços delineados no presente estudo são: (i) o desenvolvimento do PWDI, que é baseado nas características espectrais advindas da estrutura molecular dos polímeros; (ii) a identificação de plásticos submersos pelo PWDI nas imagens sintéticas do modelo DART. A aplicação desta metodologia tornou possível que plásticos submersos de 2 até 5 cm na coluna d’água pudessem ser detectados. De acordo com Moshtaghi et al. (2021), uma das principais ocorrências de falsos negativos com a aplicação do

FDI (Biermann et al., 2020) foi a qualquer nível de submersão dos plásticos abaixo da coluna d'água.

Deste modo, o presente estudo demonstra o potencial da integração entre modelos de transferência radiativa com técnicas de clusterização e aprendizado de máquina para detecção de plásticos em zonas costeiras. Ao empregar a análise das assinaturas espectrais dos plásticos e desenvolver índices radiométricos adaptados às suas características únicas, é possível melhorar a precisão e eficácia das técnicas de monitoramento de poluição por plásticos por sensoriamento remoto.

FINANCIAMENTO

Este trabalho teve por órgão financiador a CAPES através da bolsa de estudos de Mestrado.

REFERÊNCIAS

ACUÑA-RUZ, T. et al. Anthropogenic marine debris over beaches: Spectral characterization for remote sensing applications. Remote Sensing of Environment, v. 217, p. 309-322, 2018.

ALEEM, A. et al. Target Classification of Marine Debris Using Deep Learning. Intelligent Automation & Soft Computing, v. 32, n. 1, 2022.

ANDRADY, A. L. Microplastics in the marine environment. Marine pollution bulletin, v. 62, n. 8, p. 1596-1605, 2011.

ARETOULAKI, E. et al. Marine plastic littering: A review of socio economic impacts. J. Sustain. Sci. Manag, v. 16, n. 3, p. 277-301, 2021.

BALLESTEROS, L. V.; MATTHEWS, J. L.; HOEKSEMA, B. W. Pollution and coral damage caused by derelict fishing gear on coral reefs around Koh Tao, Gulf of Thailand. Marine pollution bulletin, v. 135, p. 1107-1116, 2018.

BERTELSEN, I. M. G.; OTTOSEN, L. M. Engineering properties of fibres from waste fishing nets. In: International RILEM Conference on Materials, Systems and Structures in Civil Engineering. Technical University of Denmark, Department of Civil Engineering, 2016. p. 7-16.

BIERMANN, L. et al. Finding plastic patches in coastal waters using optical satellite data. Scientific reports, v. 10, n. 1, p. 5364, 2020.

CAMPANALE, C. et al. A practical overview of methodologies for sampling and analysis of microplastics in riverine environments. Sustainability, v. 12, n. 17, p. 6755, 2020.

CIAPPA, A. C. Marine plastic litter detection offshore Hawai'i by Sentinel-2. Marine Pollution Bulletin, v. 168, p. 112457, 2021.

DE BARROS, B. M.; BARBOSA, D. G.; HACKMANN, C. L. Spectral Analysis of Marine Debris in Simulated and Observed Sentinel-2/MSI Images using Unsupervised Classification. arXiv preprint arXiv:2306.15008, 2023.

DIERSSEN, H. M.; GARABA, S. P. Bright oceans: Spectral differentiation of whitecaps, sea ice, plastics, and other flotsam. Recent Advances in the Study of Oceanic Whitecaps: Twixt Wind and Waves, p. 197-208, 2020.

GARABA, S. P.; DIERSSEN, H. M. Spectral reference library of 11 types of virgin plastic pellets common in marine plastic debris. Data Set, 2017.

GARABA, S. P.; DIERSSEN, H. M. An airborne remote sensing case study of synthetic hydrocarbon detection using short wave infrared absorption features identified from marine-harvested macro-and microplastics. Remote Sensing of Environment, v. 205, p. 224-235, 2018.

GARABA, S. P. et al. Concentration, anisotropic and apparent colour effects on optical reflectance properties of virgin and ocean-harvested plastics. Journal of Hazardous Materials, v. 406, p. 124290, 2021.

GASTELLU-ETCHEGORRY, J.; GRAU, E.; LAURET, N. DART: A 3D model for remote sensing images and radiative budget of earth surfaces. Modeling and simulation in engineering, n. 2, 2012.

GONÇALVES, G. et al. Quantifying marine macro litter abundance on a sandy beach using unmanned aerial systems and object-oriented machine learning methods. Remote Sensing, v. 12, n. 16, p. 2599, 2020.

HU, C. Remote detection of marine debris using Sentinel-2 imagery: A cautious note on spectral interpretations. Marine Pollution Bulletin, v. 183, p. 114082, 2022.

JANSEN, J. A. Plastics–It's All About Molecular Structure. Plast. Eng, 2016.

KUESTER, T.; BOCHOW, M. Spectral Modeling of Plastic Litter in Terrestrial Environments-Use of 3D Hyperspectral Ray Tracing Models to Analyze the Spectral Influence of Different Natural Ground Surfaces on Remote Sensing Based Plastic Mapping. In: 2019 10th Workshop on Hyperspectral Imaging and Signal Processing: Evolution in Remote Sensing (WHISPERS). IEEE, 2019. p. 1-7.

KÜHN, S.; BRAVO REBOLLEDO, E. L.; VAN FRANEKER, J. A. Deleterious effects of litter on marine life. Marine anthropogenic litter, p. 75-116, 2015.

MAGRINI, A. Impactos ambientais causados pelos plásticos: uma discussão abrangente sobre os mitos e os dados científicos. Editora E-papers, 2012.

MARTÍNEZ-VICENTE, V. et al. Measuring marine plastic debris from space: Initial assessment of observation requirements. Remote Sensing, v. 11, n. 20, p. 2443, 2019.

MOSHTAGHI, M. et al. Spectral reflectance of marine macroplastics in the VNIR and SWIR measured in a controlled environment. Scientific Reports, v. 11, n. 1, p. 5436, 2021.

PAPAGEORGIOU, D. et al. Sentinel-2 detection of floating marine litter targets with partial spectral unmixing and spectral comparison with other floating materials (plastic litter project 2021). Remote Sensing, v. 14, n. 23, p. 5997, 2022.

PAPINI, M. Analysis of the reflectance of polymers in the near-and mid-infrared regions. Journal of Quantitative Spectroscopy and Radiative Transfer, v. 57, n. 2, p. 265-274, 1997.

PHAM, C. K. et al. Marine litter distribution and density in European seas, from the shelves to deep basins. PloS one, v. 9, n. 4, p. e95839, 2014.

SALGADO-HERNANZ, P. M. et al. Assessment of marine litter through remote sensing: recent approaches and future goals. Marine Pollution Bulletin, v. 168, p. 112347, 2021.

SCHWARZ, A. E. et al. Sources, transport, and accumulation of different types of plastic litter in aquatic environments: a review study. Marine pollution bulletin, v. 143, p. 92-100, 2019.

TASSERON, P. et al. Advancing floating macroplastic detection from space using experimental hyperspectral imagery. Remote Sensing, v. 13, n. 12, p. 2335, 2021.

THEMISTOCLEOUS, K. et al. Investigating detection of floating plastic litter from space using sentinel-2 imagery. Remote Sensing, v. 12, n. 16, p. 2648, 2020.

TOPOUZELIS, K. et al. Remote sensing of sea surface artificial floating plastic targets with Sentinel-2 and unmanned aerial systems (plastic litter project 2019). Remote Sensing, v. 12, n. 12, p. 2013, 2020.

VANHELLEMONT, Q.; RUDDICK, K. Acolite for Sentinel-2: Aquatic applications of MSI imagery. In: Proceedings of the 2016 ESA Living Planet Symposium, Prague, Czech Republic. 2016. p. 9-13.

ZHANG, F. et al. Composition, spatial distribution and sources of plastic litter on the East China Sea floor. Science of The Total Environment, v. 742, p. 140525, 2020.